Earth-Science Reviews 218 (2021) 103684

Contents lists available at ScienceDirect

Earth-Science Reviews

journal homepage: www.elsevier.com/locate/earscirev

Magma reservoir evolution during the build up to and recovery from caldera-forming eruptions – A generalizable model?

C. Bouvet de Maisonneuve [a,*], F. Forni [a], O. Bachmann [b]

[a] Earth Observatory of Singapore and Asian School of the Environment, Nanyang Technological University, Singapore 639798, Singapore
[b] ETH Zürich, Dept. of Earth Sciences, Clausiusstrasse 25, 8092 Zürich, Switzerland

ARTICLE INFO

Keywords:
Calderas
Reservoir evolution
Chemical evolution
Polycyclic activity
Timing

ABSTRACT

Silicic calderas globally tend to record a cyclic magmatic, structural, and eruptive evolutionary progression. Some calderas are polycyclic, involving multiple catastrophic collapses in the same approximate location. Here we discuss five examples from well-studied, geologically-young and active magmatic systems: The Kos-Nisyros Volcanic Complex (Greece), Long Valley (USA), Campi Flegrei (Southern Italy), Rabaul (Papua New Guinea), and Okataina (New Zealand) in order to gain insights on the inner workings of caldera systems during the build up to and recovery from large explosive eruptions. We show that the sub-caldera magmatic system evolves through a series of processes, here collectively termed "caldera cycle", that are common to monocyclic and polycyclic calderas. In the case of polycyclic calderas, they accompany the transition from one caldera-forming eruption to the next. The caldera cycle comprises (1) the period of pre-collapse activity (incubation, maturation, widespread presence of a magmatic volatile phase), (2) the catastrophic caldera-forming (CCF) eruption, and (3) post-collapse recovery (resurgence, renewed eruptions, subsequent maturation) or the possible cessation of the cycle. The incubation phase corresponds to a period of thermal maturation of the crust, during which eruptions are frequent and of small volume due to the limited capability of reservoirs to grow. During the maturation phase, magma reservoirs gradually grow, coalesce, homogenize, magmas differentiate, and eruption frequency decreases. The system transitions into the fermentation phase once an exsolved magmatic volatile phase is continuously present in the reservoir, thereby increasing the compressibility of the magma and instigating a period of runaway growth of the reservoir. A CCF eruption at the end of the fermentation phase could be the concatenated result of multiple magmatic processes (including magma recharge, volatile exsolution, and crystal mush remelting) pressurizing the reservoir, while external factors (e.g., tectonic processes) can also play a role. Postcaldera eruptions, subvolcanic intrusions, and hydrothermal activity typically continue, even if the magma supply wanes. If, however, magma supply at depth remains substantial, the system may recover, initially erupting the remobilized remains of the CCF reservoir and/or new recharging magmas until a shallow reservoir starts to grow and mature again. Placing other calderas worldwide within this framework would enable to test the robustness of the proposed framework, deepen the understanding of what controls the duration of a cycle and its individual phases, and refine the petrologic, geophysical, and unrest symptoms that are characteristic of the state of a system.

1. Introduction

Volcanic unrest, particularly in areas that have experienced catastrophic caldera-forming (CCF) eruptions in the past, creates important dilemmas for hazard assessment, as many episodes of unrest do not lead to an eruption and few eruptions are caldera-forming (Newhall and Dzurisin, 1988). The inherent difficulty is that the "brewing time" to grow subvolcanic reservoirs to gigantic sizes (up to several thousands of km^3) may take 10s to 100s of thousands of years to millennia but the evacuation time is typically much shorter (i.e., on the order of days). During the growth stage of caldera-related magma reservoirs, countless "unrest episodes" happen, likely recording recharge events in their subvolcanic storage zone, but few of those unrest episodes have major consequences on people living around the volcano. The ground may deform and shake, hot gases may vent more vigorously, but then the system falls back to sleep (e.g. Campi Flegrei in the 1970s and 1980s,

* Corresponding author.
E-mail addresses: carolinebouvet@ntu.edu.sg (C. Bouvet de Maisonneuve), fforni@ntu.edu.sg (F. Forni), olivier.bachmann@erdw.ethz.ch (O. Bachmann).

https://doi.org/10.1016/j.earscirev.2021.103684
Received 4 November 2020; Received in revised form 11 May 2021; Accepted 14 May 2021
Available online 17 May 2021

Rabaul in the 1980s, Nisyros in the 1990s, Taal in 2020) and little or no magma reaches the surface. Even if small amounts erupt from time to time (for example, Monte Nuovo in 1538 CE at Campi Flegrei, Italy or Rabaul, Papua New Guinea in 1994), climactic eruptions of 10s to 100s or even 1000s of km^3 volume are rare, and interpreting possible signs of an impending major caldera-forming event can be challenging for the volcanological community. Hence, understanding the magmatic processes occurring beneath silicic calderas and relating them to the patterns of unrest remains a major goal in volcanology.

Silicic caldera-forming eruptions are often preceded by mafic to silicic eruptions, and followed by activity that can be resurgent (i.e., uplift of the caldera floor) or magmatic (i.e., intrusion or eruption along the collapse faults) (Lipman, 2000). Some magmatic systems around the world have produced multiple caldera-forming eruptions in the same approximate location (i.e., nested calderas). For example, the Yellowstone Plateau volcanic field (USA) erupted three major ignimbrite sheets during the last 2.1 Myr (Christiansen, 2001). Lake Toba in northern Sumatra (Indonesia) produced at least three caldera forming eruptions, the last of which (the Youngest Toba Tuff; ~74 ka) is the largest eruption in the Quaternary (Knight et al., 1986; Chesner and Rose, 1991; Chesner et al., 1991). Thus, it is likely that a number of volcanic systems in the world have the potential to produce a future large caldera-forming eruption (Newhall and Dzurisin, 1988).

Although countless studies have applied field, petrologic, geochronologic, and geophysical data to ignimbrite caldera processes, several questions remain unresolved. For example: *What are the long- and short-term precursors of a caldera-forming eruption? When is the transition from post-caldera (recovery) activity to pre-caldera (precursory) activity and how does it occur? What controls the recurrence intervals between caldera-forming eruptions? How to interpret signs of unrest?* In order to bring elements of answers to these questions, we further the concept of a generalized 'caldera cycle', as earlier proposed by Smith and Bailey (1968), Lipman (1984, 2000) and Cole et al. (2005), to include the detailed temporal evolution of the state and properties of the subvolcanic system. The caldera cycle, whether for mono- or polycyclic systems, comprises (1) the period of pre-collapse activity (incubation, maturation, exsolution of a widespread magmatic volatile phase), (2) the catastrophic caldera-forming (CCF) eruption, and (3) post-collapse recovery (resurgence, renewed eruptions, subsequent maturation) or the possible cessation of the cycle. Unlike previous studies, however, we view the onset of incubation or recovery from a previous CCF eruption as the onset of the caldera cycle and the occurrence of the CCF eruption as the end of a caldera cycle. The duration of a full caldera cycle thus corresponds to the repose time between two CCF eruptions. We use the term CCF eruption to distinguish a violently explosive eruption of substantially (one or more orders of magnitude) larger volume than the usual, average eruption volume of a given system.

This paper discusses specificities of the caldera cycle based on the chronology and magmatic compositions at five well-studied, geologically-young and active magmatic systems: Kos-Nisyros (Greece), Long Valley (CA, USA), Campi Flegrei (Italy), Rabaul (Papua New Guinea), and Okataina (New Zealand). The initial intent was to review more such well-studied caldera complexes in order to also gain insights into the duration of the caldera cycle and the influence of tectonic setting, but this has proven to be challenging. The incompleteness of petrologic data for many systems limits the interpretive approach we propose. The timescales for the stages of magmatism and the conditions that precede most CCF eruptions are insufficiently known despite many studies. This could be due to the challenges associated with studying inter-caldera eruptions that are smaller, often less well preserved, and potentially harder to date, in addition to being less glamourous (as less hazardous). We hope that expanded datasets will develop to test the model and strengthen our understanding of the topic. Identifying the common points in the evolution of ignimbrite caldera systems is essential for a better assessment of volcanic hazards at active calderas.

2. Case studies

2.1. Kos-Nisyros Volcanic Complex

The Kos-Nisyros Volcanic Complex; Fig. 1) has been active for more than 3 My and is a result of the South African plate subducting beneath the Aegean microplate (Fytikas et al., 1976; Bachmann et al., 2010). Its volcanic activity culminated 161 ky ago (Fig. 2; Smith et al., 1996; Guillong et al., 2014) in a caldera-forming eruption that ejected >60 km^3 DRE of pumice and ash, producing the Kos Plateau Tuff (Allen, 2001). Post-Kos Plateau Tuff magmatic activity built the islands of Nisyros and Yali. The youngest phreatic eruption occurred in 1888 CE (Groceix, 1873; Dietrich and Lagios, 2018) while the latest magmatic eruption is around 20 ka (Popa et al., 2020), both from Nisyros. Two post-Kos Plateau Tuff explosive eruptions, the Lower and Upper Pumice, were caldera-forming and produced the 4 km wide depression at the summit of Nisyros. However, these are not considered to be CCF eruptions as they are at least one order of magnitude less voluminous than the Kos Plateau Tuff and of similar volume as other pre- and post-Kos Plateau Tuff eruptions with no associated calderas (Dietrich and Lagios, 2018; Popa et al., 2019). The Kos-Nisyros Volcanic Complex may not be an ideal location to discuss caldera cycles as it has limited age constraints (problems with excess Ar in the old eruptive units, absence of charcoal for radiocarbon dating in the young deposits (Volentik et al., 2005; Zellmer and Turner, 2007; Bachmann et al., 2010)), and is mostly under water thereby yielding few outcrops to study. However, it has been the subject of detailed petrologic and geochemical studies for over forty years (Di Paola, 1974; Wyers and Barton, 1989; St Seymour and Vlassopoulos, 1992; Vougioukalakis, 1993; Dabalakis and Vougioukalakis, 1993; Buettner et al., 2005; Pe-Piper et al., 2005; Bachmann et al., 2007; Zellmer and Turner, 2007; Francalanci et al., 2007; Braschi et al., 2012, 2014; Dietrich and Popa, 2018), the relative and absolute ages of eruption are increasingly well constrained (Guillong et al., 2014; Popa et al., 2020), and a growing number of studies have considered the system as a whole, linking the various volcanic centers and deposits in a common magmatic framework (Di Paola, 1974; Pe-Piper and Moulton, 2008; Bachmann, 2010; Piper et al., 2010; Bachmann et al., 2012, 2019; Dietrich and Popa, 2018; Popa et al., 2019). The occurrence of only one CCF eruption also presents the advantage of enabling to reconstruct the early history of the system, from the initiation of magmatism to the (first) CCF eruption, something that is not possible where multiple CCF eruptions have occurred, obliterating the early eruption record (e.g. Campi Flegrei, Rabaul or Okataina).

2.2. Long Valley caldera

The Long Valley caldera and its associated volcanic field are located in the Owens Valley Rift in central eastern California, straddling the Sierra Nevada and western Basin and Range provinces (Fig. 1). Volcanic activity in the area initiated 4–4.5 My ago (Moore and Dodge, 1980), shortly after the onset of rifting (Larson et al., 1968; Ward, 1991), and culminated 765 ky ago (Andersen et al., 2017) with the eruption of the ~650 km^3 Bishop Tuff that produced the Long Valley caldera (Fig. 3; Hildreth, 1979). Post-caldera magmatic activity continued in the center of the caldera and then to the west and northwest producing a vast array of mafic to silicic vents. The youngest eruptive episode in the region was rhyolitic and occurred in the 14th century from the Mono and Inyo volcanic chains (Sieh and Bursik, 1986; Bursik et al., 2014). The Long Valley system is well-documented and extensively dated, providing an excellent example of evolution from the onset of magmatism to the (first) CCF eruption. As for the Kos-Nisyros Volcanic Complex, the system has only experienced one CCF eruption, which is why the early magmatic activity is preserved in the geologic record. Although it hasn't been previously studied and interpreted within a framework of caldera cycles per se, its temporal evolution has been described in detail (e.g. Bailey, 2004; Hildreth, 2004) and it has the advantage over the Kos-

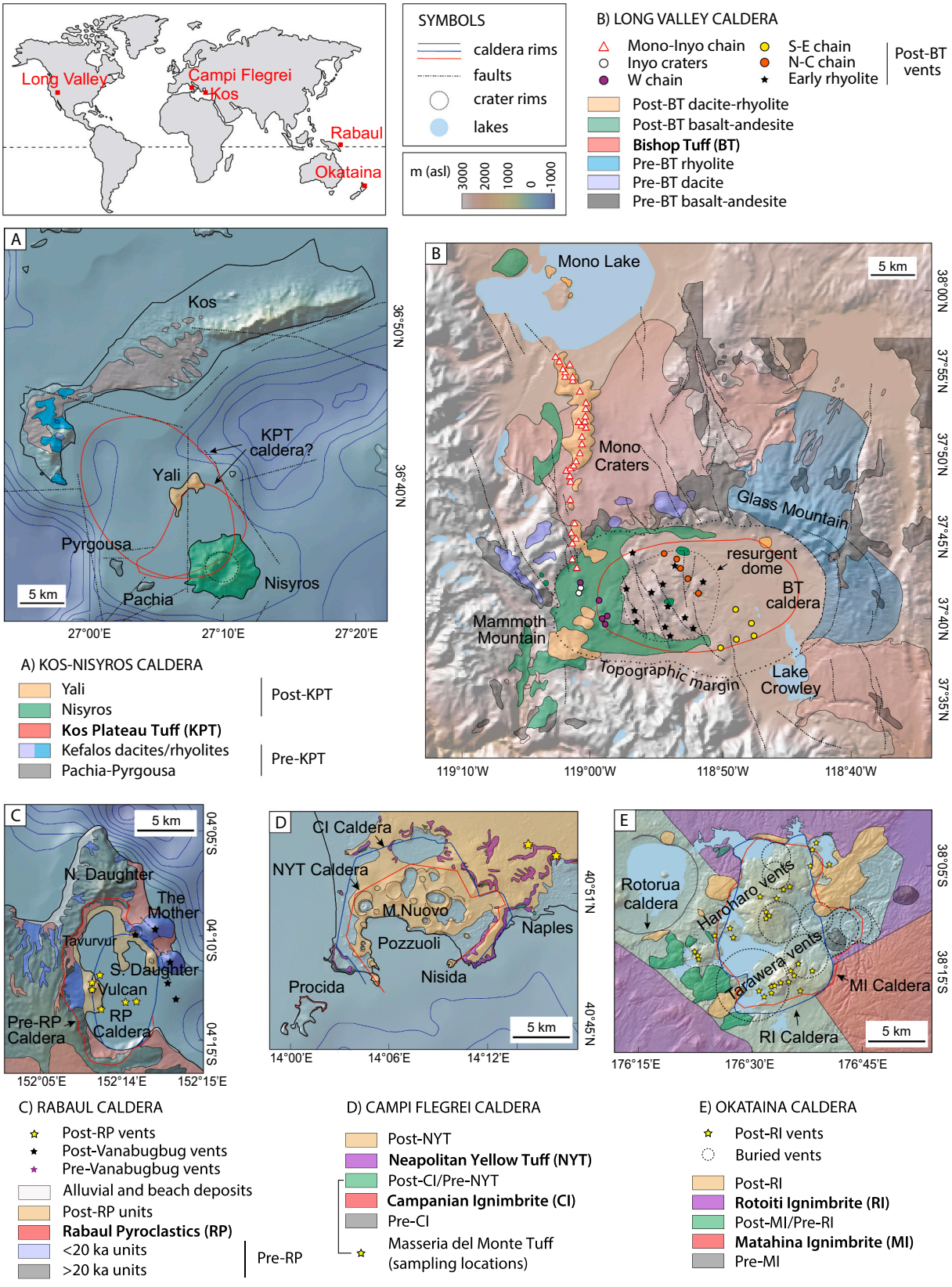

Fig. 1. Location and simplified geologic maps of the five case studies: (A) The Kos-Nisyros Volcanic Complex, (B) Long Valley, (C) Rabaul, (D) Campi Flegrei, and (E) Okataina. The distribution of vents and deposits is from (Nairn et al., 1989; Pappalardo et al., 1999; Bailey, 2004; Hildreth, 2004; Deering et al., 2011b; Cole et al., 2014; Bachmann et al., 2019). Deposits related to catastrophic caldera-forming (CCF) events are in red or purple while deposits from inter-caldera eruptions are colour-coded by age/time period from gray, blue, green, to yellow. (For interpretation of the references to colour in this figure legend, the reader is referred to the web version of this article.)

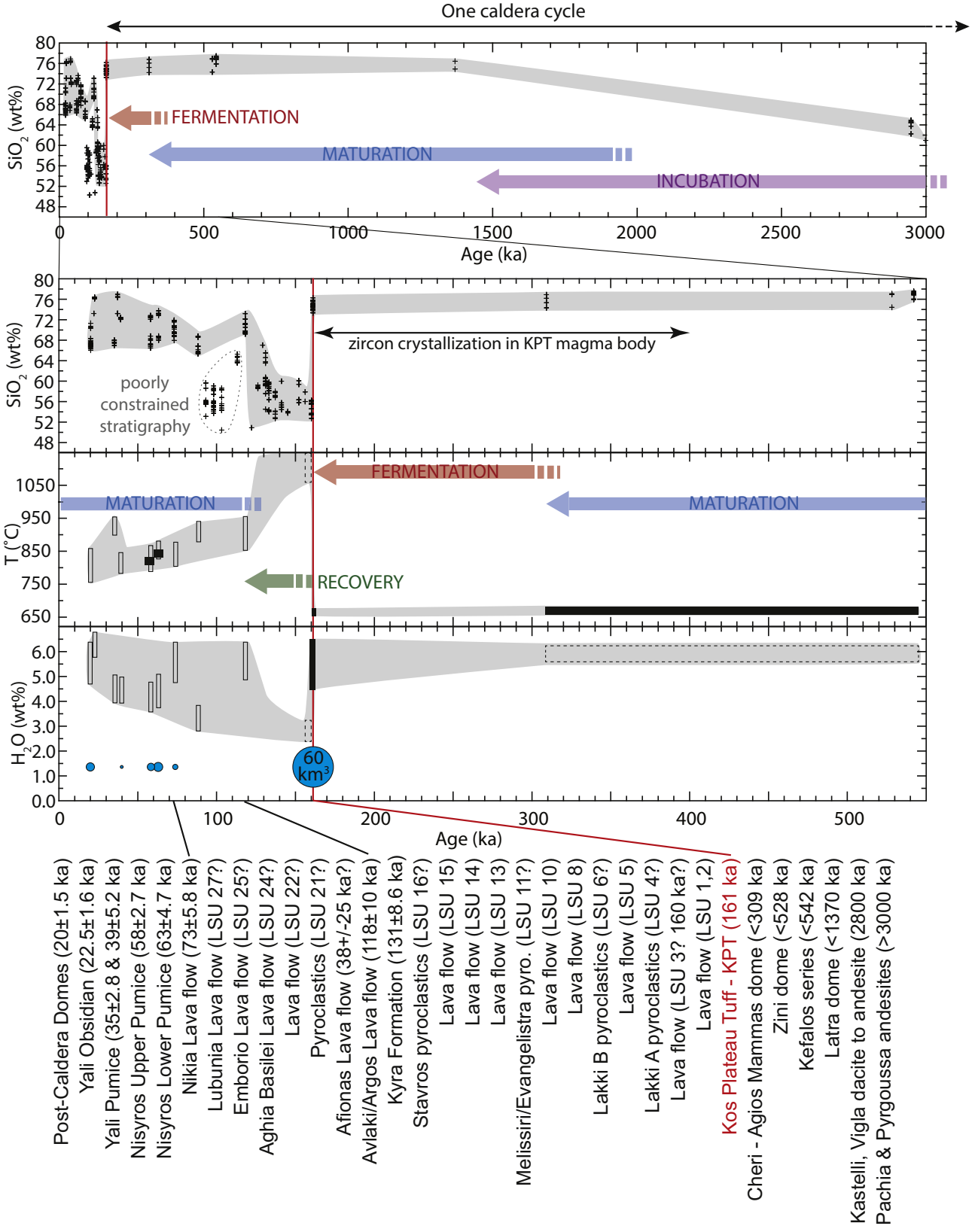

Fig. 2. Temporal evolution of magma compositions (bulk rock SiO_2 content), pre-eruptive temperatures and water contents at the Kos-Nisyros Volcanic Complex. When known, erupted volumes of individual eruptions (Dietrich and Lagios, 2018) are shown with blue circles of scaled area. Purple, blue, red and green arrows indicate the timings of the incubation, maturation, fermentation, and recovery phases, respectively. Bulk rock SiO_2 contents are from the data compilation of Dietrich and Popa (2018). Temperature and H_2O contents are from Popa et al. (2019) for the evolved Nisyros and Yali units, and Bachmann et al. (2012) for the KPT and pre-KPT units. Temperature and H_2O contents for the early mafic units of Nisyros were computed from the data of Spandler et al. (2012) using the clinopyroxene-liquid (whole-rock composition in this case) geothermometer of Putirka (2008) and the plagioclase hygrometer of Waters and Lange (2015). Zircon crystallization ages are from Bachmann et al. (2007). (For interpretation of the references to colour in this figure legend, the reader is referred to the web version of this article.)

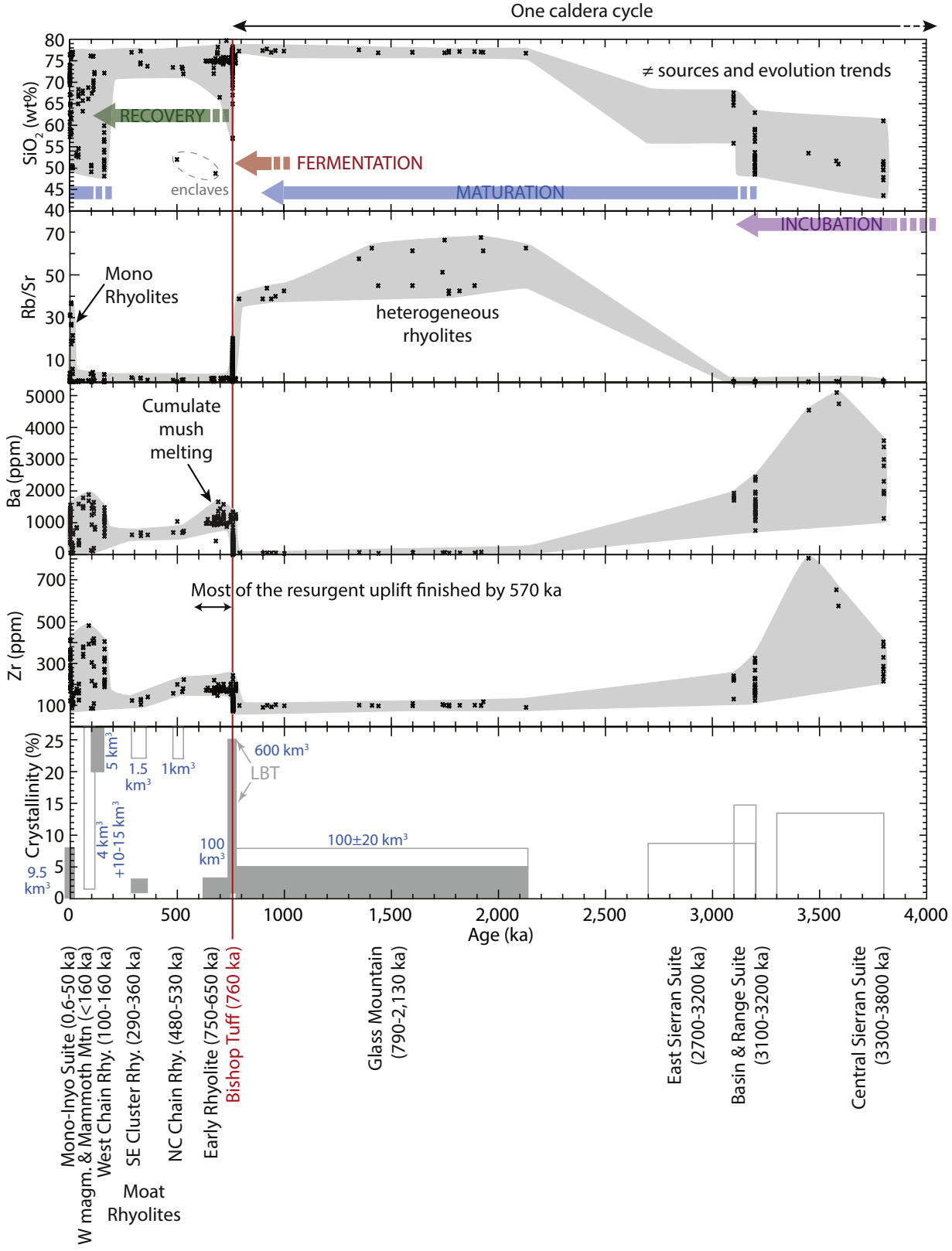

Fig. 3. Temporal evolution of magma compositions (bulk rock SiO_2, Rb/Sr, Ba, and Zr contents) and crystal content at Long Valley caldera. Notice the particularly high Ba and Zr contents in the Early Rhyolite, that we interpret as post-Bishop Tuff cumulate mush melting. When known, erupted volumes for the various eruptive episodes are labeled in blue next to the average crystal content of magmas from the same episode. Purple, blue, red and green arrows indicate the timings of the incubation, maturation, fermentation, and recovery phases, respectively. Data is from Metz and Mahood (1991), Bailey (2004), Hildreth and Wilson (2007), Van Kooten (1980), Hildreth (2017), Heumann and Davies (1997), Sampson and Cameron (1987), and Kelleher and Cameron (1990). Duration of the resurgent uplift is from Hildreth et al. (2017). LBT = Late Bishop Tuff. (For interpretation of the references to colour in this figure legend, the reader is referred to the web version of this article.)

Nisyros Volcanic Complex of being wholly subaerial and easier to date, thereby providing a more complete record of magmatic volumes and evolution.

2.3. Campi Flegrei

Campi Flegrei is a polycyclic caldera located in the Campanian Plain (Southern Italy), an area that has been affected by crustal extension since the Pliocene due to the opening of the Tyrrhenian back arc basin behind the Apennine subduction zone (e.g. Scandone and Patacca, 1984). The onset of magmatic activity at Campi Flegrei is unknown; the oldest volcanic rocks in the area date back to ~60 ka and refer to eruptive centers located outside the present caldera (Pappalardo et al., 1999) (Fig. 1). The Campi Flegrei caldera sourced at least two catastrophic eruptions, the Campanian Ignimbrite, ~40 ka (Giaccio et al., 2017)) and the Neapolitan Yellow Tuff, ~15 ka (Deino et al., 2004), that produced ~200 and ~40 km^3 of trachyphonolitic magma (DRE), respectively (Fig. 4). The volcanic activity between the two caldera-forming eruptions (pre-Neapolitan Yellow Tuff) was mainly characterized by small and frequent eruptions from volcanic centers located inside and close to the rims of the Campanian Ignimbrite caldera (Pappalardo et al., 1999) (Fig. 1). A third large eruption (Masseria del Monte; ~16 km^3 DRE), although not associated with an exposed collapsed structure, has been recently identified at Campi Flegrei and dated at 29.3 ka (Albert et al., 2019). The estimated volume and magnitude of this eruption are based on the correlation between the proximal deposits with the tephra layer Y3 that covers an area of >150,000 km^2 in the Mediterranean region. Since the Neapolitan Yellow Tuff eruption, Campi Flegrei caldera has been the site of more than 60 small eruptions (<1 km^3 DRE) divided into three epochs of activity (Fig. 4). The most recent eruption, Monte Nuovo at 1538 CE (Di Vito et al., 1987) has marked the beginning of a new period of quiescence characterized by fumarolic activity and several episodes of ground deformation (Chiodini et al., 2016; Kilburn et al., 2017). Stratigraphic and geochronological reconstructions of the evolution of the Campi Flegrei magmatic system during the last 60 ka are some of the most detailed that exist (Forni et al., 2018 and references therein) and thus provide a robust time-constrained petrological framework to analyze the phases of activity that lead up to and follow a CCF eruption.

2.4. Rabaul caldera

The Rabaul caldera is a 7–10 km-diameter polycyclic caldera in Papua New Guinea (Fig. 1; Nairn et al., 1995). Volcanism in the region is related to the subduction of the Solomon Sea Plate below the South Bismarck Plate (Tregoning et al., 1999). The onset of magmatic activity at Rabaul is unknown, but mafic stratovolcanoes surrounding the present caldera (Fig. 1) date back to 100–500 ka (Nairn et al., 1995; McKee and Duncan, 2016). Rabaul is the locus of at least four and possibly up to nine ignimbrite eruptions in the past 18,000 years (Nairn et al., 1995; McKee and Duncan, 2016). The most recent caldera-forming ignimbrite is the 11 km^3 (uncompacted volume) Rabaul Pyroclastics, dated at 667–699 CE by radiocarbon (Fig. 5; McKee et al., 2015). The penultimate recognized caldera-forming eruption produced the ~10.5 ka Vunabugbug Ignimbrite with an uncompacted volume of 3–5 km^3 (Nairn et al., 1995; McKee and Duncan, 2016), excluding distal tephra fall deposits. Between these two eruptions, the ~4 ka Memorial Ignimbrite, with a volume of at least 1 km^3, is likely a third recent caldera-forming eruption (Fabbro et al., in prep). Its volume is poorly constrained as the deposit has not been correlated with other proximal deposits or distal tephra. Post-Rabaul Pyroclastics eruptions have been along the ring fault. The most recent episode, from 1994 to 2014, is a rare example of simultaneous eruptions from vents on opposite sides of the caldera (Vulcan and Tavurvur) (Williams, 1995; Patia et al., 2017; Mckee et al., 2018). Two small stratovolcanoes on the NE caldera rim are rare pre-Rabaul Pyroclastics vents, and others were likely obliterated by the Rabaul Pyroclastics caldera collapse. Pre-Vunabugbug deposits are largely buried by more recent eruptions, and potential intra-caldera deposits are submerged beneath Blanche Bay. Nevertheless, Rabaul is a good example of high-frequency but small-volume caldera-forming eruptions, and its temporal evolution has been studied in detail (Nairn et al., 1995; Wood et al., 1995; McKee et al., 2015; McKee and Duncan, 2016; McKee and Fabbro, 2018). It is also a rare case example of intense caldera unrest (1970s to 1994) followed by eruptions (1994–2014) that provide a snapshot of the current state of the magma system (Bouvet de Maisonneuve et al., 2015; Fabbro et al., 2020).

2.5. The Okataina Volcanic Centre

The Okataina Volcanic Centre is a polycyclic caldera that lies at the northern end of the central Taupo Volcanic Zone on the North Island of New Zealand (Fig. 1; Cole et al., 2014). It is part of the most frequently active and productive Quaternary silicic system on Earth (Houghton et al., 1995). Volcanism in the area is a result of active rifting and westward subduction of the Pacific Plate beneath the Australian Plate (Cole, 1990; Wilson et al., 1995). Rhyolitic volcanism at Okataina may have started as early as ~625 ka (Cole et al., 2014). Okataina is home to three major caldera-forming eruptions (Fig. 6). The earliest occurred ~557 ka (Leonard et al., 2010) and produced the poorly-exposed, ~90 km^3 Utu Ignimbrite (Nairn, 2002; Deering et al., 2011b). The second occurred ~322 ka (Leonard et al., 2010) and is associated with the >160 km^3 Matahina Ignimbrite (Deering et al., 2011b). The most recent occurred ~46 ka (Danišík et al., 2012; Flude and Storey, 2016) and produced the >100 km^3 Rotoiti Ignimbrite (Nairn, 2002; Shane et al., 2005). Throughout the history of Okataina, intra- and extra-caldera rhyolite domes have been extruded, accompanied by localized block-and-ash flows and periodic Plinian eruptions (Cole et al., 2010). Evidence for pre-Utu rhyolitic eruptions exists as distal tephra layers (Manning, 1996) and angular lithic blocks within the Utu ignimbrite (Cole et al., 2014). Domes to the SW, NW, and NE of Okataina and the Murupuru Pyroclastics Subgroup were erupted post-Utu but pre-Matahina (Manning, 1996; Deering, 2009; Cole et al., 2010; Deering et al., 2011b). Following the Matahina CCF eruption, the Onuku Pyroclastics, the Pokopoko Pyroclastics, a number of rhyolite domes, and the immediately pre-Rotoiti, basaltic Matahi Scoria were emplaced (Cole et al., 2010, 2014). The Rotoiti CCF eruption was directly followed by the Earthquake Flat Pyroclastics, and then the Mangaone tephra sequence (45–28 ka; Jurado-Chichay and Walker, 2000) and young (<25 ka) lava domes erupted from two sub-parallel NE trending vent zones (the northern Harorharo and southern Tarawera vent zones) that transect the caldera complex (Cole et al., 2010). The most recent eruptions were the rhyolitic Kaharoa eruption in 1314 CE (Nairn et al., 2004) and a basaltic fissure eruption in 1886 CE, from the same segment of Tarawera vents (Sable et al., 2006). Although this system has been extensively studied, there are little to no petrologic investigations of most of the inter-CCF deposits (except for the post-Rotoiti eruptions) and the magmatic conditions that led to the Utu ignimbrite are unknown. Nevertheless, the short-term build-up to and recovery from the Rotoiti and Matahina CCF eruptions provides valuable insights into the caldera cycle concept.

3. Temporal evolution of sub-caldera reservoirs

Calderas are produced by any form of roof collapse into a large underlying shallow magma reservoir. Rather than the many mechanisms of roof collapse that have been recognized (Lipman, 2000; reviews by Cole et al., 2005), this contribution focuses on the magma dynamics within the Earth's (upper) crust that led to the formation of a magma reservoir, whose properties and/or storage conditions enable CCF eruptions to occur. It focuses on silicic calderas (andesitic to rhyolitic or their alkaline equivalents), as the collapse mechanisms of basaltic systems can be the result of effusive eruptions during which magma is drained from a

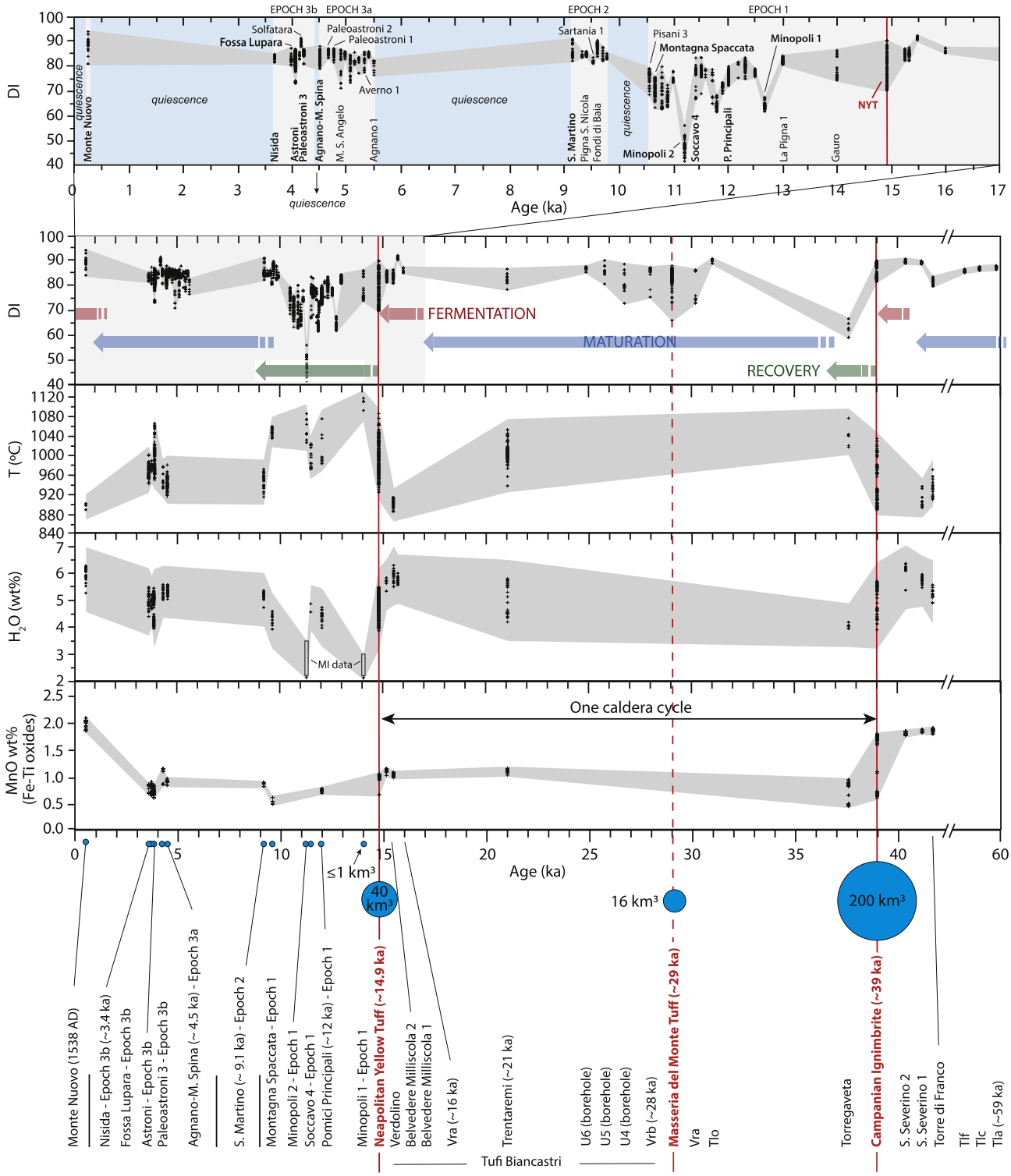

Fig. 4. Temporal evolution of magma compositions (Differentiation Index, DI = Q + Ab+Or + Ne + Lc normative), pre-eruptive temperatures and water contents, and MnO contents in titanomagnetites at Campi Flegrei. Blue, red and green arrows indicate the timings of the maturation, fermentation, and recovery phases, respectively, assuming that the Masseria del Monte tuff was not a CCF eruption. Geochemical data and volume estimates are from the compilation of Forni et al. (2018) and Albert et al. (2019). (For interpretation of the references to colour in this figure legend, the reader is referred to the web version of this article.)

lateral fissure and the roof then collapses in response to decompression in the reservoir. This does not occur when more viscous magmas are involved (Cole et al., 2005). Furthermore, this review focuses on large silicic calderas (>5 km in diameter) for which caldera collapse is controlled by ring faults. In these systems, pre- and post-collapse volcanic activity dominantly occurs from vents that are aligned along the caldera ring fault (e.g. Long Valley caldera, USA (Hildreth, 2004); Rabaul, Papua New Guinea (Roggensack et al., 1996; Jones and Stewart, 1997)) and sometimes progressively migrates towards the center (e.g. Campi Flegrei; Rivalta et al., 2019). Smaller calderas on the other hand, correspond to the collapse of a unique but large volcanic edifice (e.g. Crater Lake, Oregon (Bacon, 1983; Suzuki-Kamata et al., 1993);

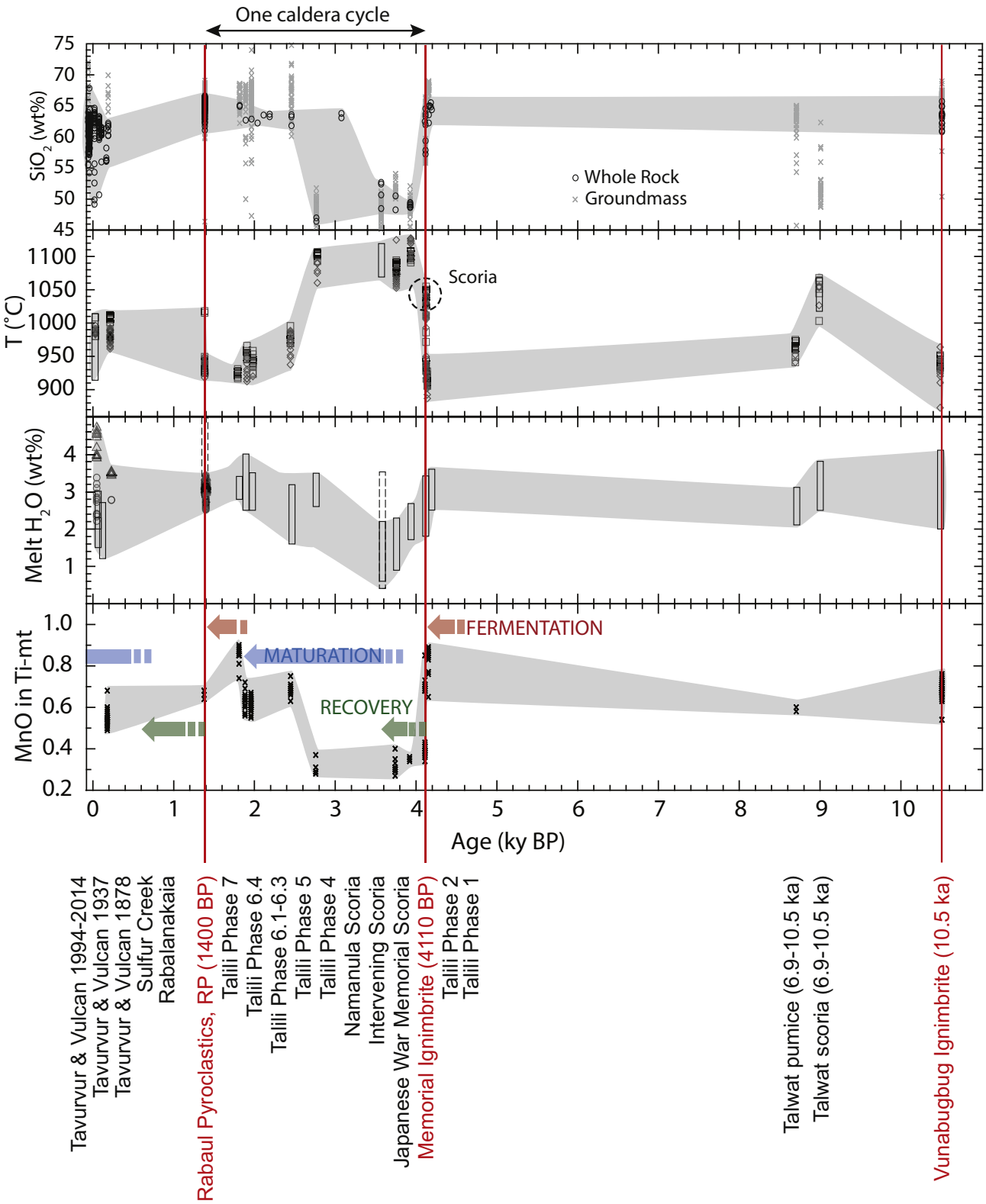

Fig. 5. Temporal evolution of magma compositions (bulk rock and groundmass SiO_2 content), pre-eruptive temperatures and water contents, and MnO contents in titanomagnetites at Rabaul. Blue, red and green arrows indicate the timings of the maturation, fermentation, and recovery phases, respectively. Data is from the compilation of Fabbro et al. (in prep). The relative age of the Talwat scoria and pumice is unknown. (For interpretation of the references to colour in this figure legend, the reader is referred to the web version of this article.)

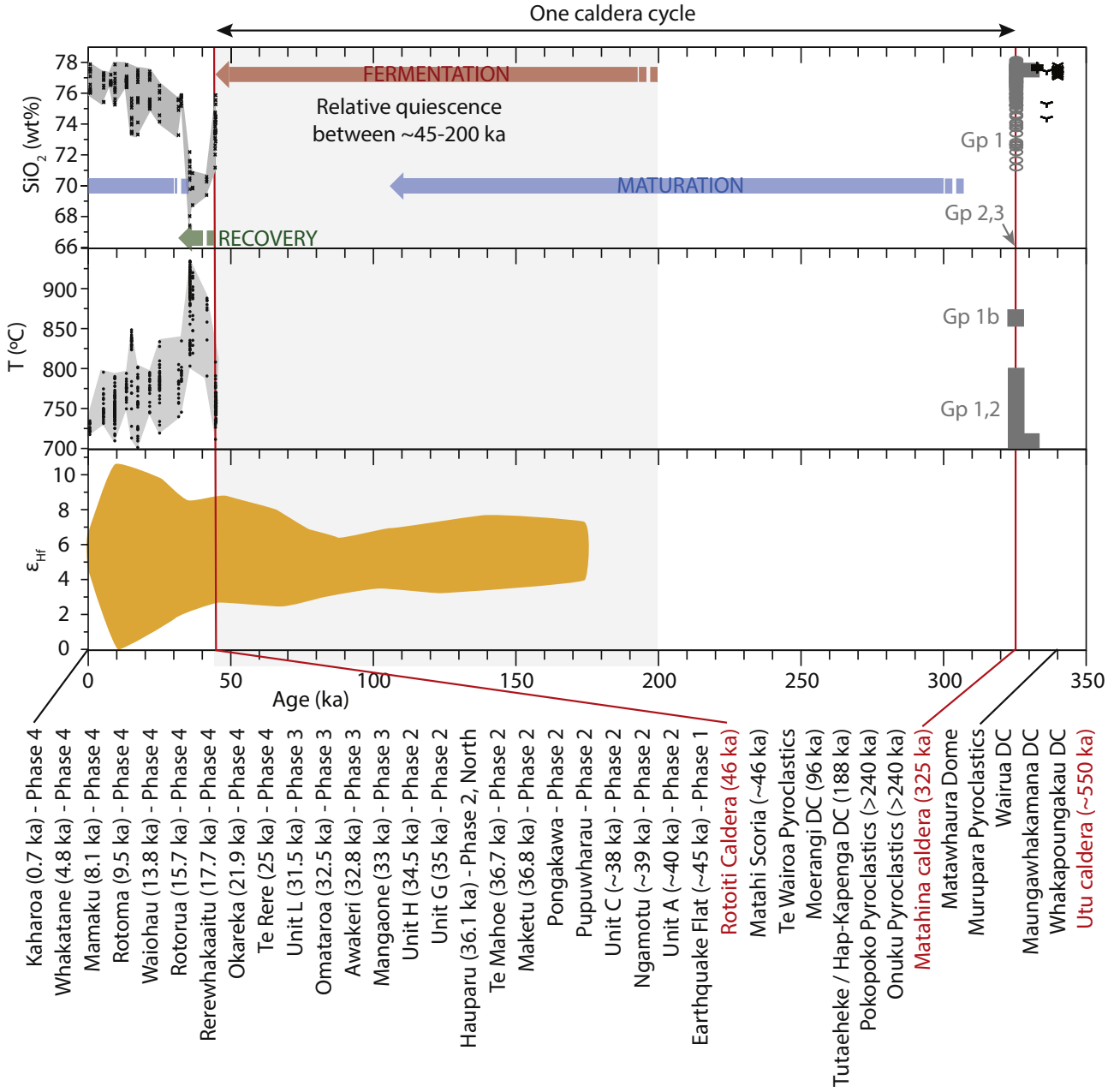

Fig. 6. Temporal evolution of magma compositions (bulk rock SiO_2 content), pre-eruptive temperatures and water contents, and zircon ε_{Hf} values at Okataina. Blue, red and green arrows indicate the timings of the maturation, fermentation, and recovery phases, respectively. Data is from Shane and Smith (2013) for the Rotoiti and post-Rotoiti eruptions, from Deering et al. (2011b) for the Matahina and pre-Matahina eruptions, and from Rubin et al. (2016) for the zircon ε_{Hf} values. (For interpretation of the references to colour in this figure legend, the reader is referred to the web version of this article.)

Tambora (Self et al., 1984) and Krakatau, Indonesia (Self and Rampino, 1981)). Pre- and post-collapse volcanic activity occurs from vents that are exclusively centrally located within the caldera. The collapse mechanisms could be significantly different, and the conditions for failure and caldera-formation may vary.

The sub-caldera magmatic system evolves through a series of magmatic, unrest and volcanic processes, here collectively termed the caldera cycle, that are common to single or polycyclic calderas (Table 1). In the case of polycyclic calderas, they accompany the transition from one caldera-forming eruption to the next (Fig. 7). The different phases of the cycle are presumably common to many calderas around the world, as they reflect the physical and thermo-mechanical evolution of the reservoir(s), from its gradual building to the emptying of most (or all) of its eruptible material with crystallinities $\leq$ ~50 vol% during a CCF eruption. The different phases include the period of pre-collapse activity (incubation, maturation, formation of a magmatic volatile phase), the series of events that trigger the CCF eruption (i.e. dynamics of reservoir pressurization or roof instability), and the period of post-collapse recovery (resurgence, renewed magmatic activity, subsequent maturation) or cessation of the cycle.

3.1. *Incubation: thermal maturation of the crust*

The formation of a silicic caldera requires the presence of a large and shallow magma reservoir, i.e. a large volume of magma with variable amounts of melt. This in turn requires the presence of thermally mature wall rocks that have a low effective viscosity (Jellinek and DePaolo, 2003; de Silva and Gosnold, 2007; Gregg et al., 2012; de Silva and

Table 1
Summary of the internal and surficial characteristics of the different phases of the Caldera Cycle.

Phase of the Caldera Cycle	Upper crustal reservoir processes and characteristics	Petrological/geochemical characteristics of eruptive products	Likely eruptive activity and/or surface manifestations
Incubation	Network of small dikes/sills, with few to no associated long-lived storage zones of evolved magma. Thermal maturation of the crust starts.	Basalts to andesites/dacites (or their alkaline counterparts), poorly differentiated, typically rather hot and dry.	Distributed mafic to intermediate volcanism (stratovolcanoes, cones). Frequent but small volume eruptions.
Maturation	Development of a single or multiple reservoir(s), growing in size (and possibly merging), increasing differentiation and volatile contents, transient presence of an exsolved magmatic volatile phase, development of a crystal mush.	Dominantly dacites to rhyolites (or their alkaline counterparts), signs of increasing degrees of differentiation, low-pressure storage, decreasing magma storage temperature, increasing volatile contents.	Distributed intermediate to silicic volcanism. Initially high but decreasing eruptive frequency. Obsidian flows or (sub)plinian eruptions can appear.
Fermentation	Presence of one or more long-lived reservoir(s), continuous presence of an exsolved magmatic volatile phase, runaway reservoir growth and increasing capture radius of recharging magmas. Potential formation of a large, melt-rich cap on the dominantly mushy reservoir.	Most evolved magmas observed in the system's eruptive history, coolest, crystal-poorest, and most volatile-rich. Ignimbrite from the CCF eruption involving crystal-rich, rejuvenated mush material or a melt-rich cap with its remobilized, crystal-rich cumulative counterpart.	Infrequent eruptions of very silicic magma. Large scale unrest as deformation, seismic swarms, bradiseismic activity, very active hydrothermal system. Culminates in a CCF eruption.
Recovery	Following CCF eruption, silicic material and volatiles have been largely evacuated; recharging mafic to intermediate magmas regain greater influence on shallow magma reservoir(s), bringing heat and new material, and melting remnants (if low-temperature or hydrous mineral phases are present).	Return to less evolved, hotter and dryer magmas. Left over magma from the CCF eruption, with signs of cumulate melting and/or renewed mass addition.	Distributed volcanism. Composition depends on how extensively the upper crustal reservoir was tapped but is typically less homogeneous. Structural resurgence.
Death of the caldera cycle	No development of a large upper crustal magma reservoir, as deep recharge flux wanes.	Magmas of potentially varied composition but no indications of abundant magma recharge.	Distributed volcanism with low/average eruptive frequency. Plutonic trapping dominates.

Gregg, 2014; Degruyter and Huber, 2014). Thermal models have shown that prolonged mafic intrusion in the lower crust (over timescales of 10^5 to 10^6 years), promotes the development and sustenance of upper crustal magma reservoirs (Karakas et al., 2017). In the absence of such a thermally mature crust, magmas erupt shortly after emplacement or freeze in-situ, thus not allowing reservoir growth or long-term magma storage and differentiation (Townsend et al., 2019). Magmatic activity at a future caldera site starts with an incubation or "preheating" phase during which mafic volcanism is geographically dispersed (Fig. 7a). Basalts to andesites or their alkaline equivalent typically erupt during the incubation period, as small reservoirs in the upper crust do not permit extensive magmatic differentiation. As the pre-existing crust is progressively heated by the mafic magmas transiting through it, larger reservoirs are able to build, and magmas differentiate.

At the Kos-Nisyros Volcanic Complex for example, andesitic volcanism started on the island of Pachia before 3 Ma, followed by dacitic activity on the Kefalos peninsula on Kos at ~2.95 Ma (Figs. 1, 2), while the CCF eruption of the Kos Plateau Tuff only occurred at ~161 ka (Bachmann et al., 2019). Similarly, at Long Valley, the first leaks of mafic magma from the mantle started approx. 4.5 Ma, and the basaltic volcanism of the Basin and Range and East Sierran suites reached dacitic compositions around 2.7–3.1 Ma (Bailey, 2004; Hildreth, 2004), while the CCF eruption of the Bishop Tuff only occurred 765 ka (Figs. 1, 3). A time span of up to ~1 Ma between the onset of volcanism and the appearance of differentiated magmas (dacites) that involve more prolonged storage in crustal reservoirs is consistent with the thermal modelling of Karakas et al. (2017). Once thermal diffusion has sufficiently lowered the effective viscosity of the crust and larger reservoirs are able to form, the system transitions to the maturation phase.

3.2. *Maturation: reservoir growth and magma differentiation*

The maturation phase corresponds to a period of magma differentiation and accumulation. Pre-collapse volcanism evolves from mafic (produced during the incubation or recovery phase) to evolved magmas (i.e. dacites and rhyolites or phonolites and trachyphonolites) that form the pre-caldera erupted magmas and the CCF tuff (Fig. 7b–c). At the Kos-Nisyros Volcanic Complex, the Kefalos dacitic eruptions transitioned to rhyolitic effusive and explosive eruptions around 1.5 Ma to 550 ka (Fig. 2). At Long Valley, the dacitic magmatism of the Basin and Range and East Sierran suites gave place to the voluminous Glass Mountain rhyolites, around 2.2 Ma (Fig. 3). At Campi Flegrei the magmas evolved from basaltic trachyandesites following the Campanian Ignimbrite to trachyphonolites preceding the Neapolitan Yellow Tuff (Forni et al., 2018; Fig. 4). And at Rabaul, magmas evolved from basalts following the Memorial Ignimbrite to dacites before the Rabaul Pyroclastics (Fig. 5). As the magma reservoir(s) grow and/or coalesce, the volume of silicic magma increases, and mafic magmas ascending from the lower crust or mantle are incorporated within the system or stall at a lower level beneath the more evolved magmas (Karlstrom et al., 2009; Degruyter and Huber, 2014; Pansino and Taisne, 2019; Fabbro et al., 2020). Evidence for mafic magma replenishment in the erupted products becomes either rarer or subtler. For example, mafic recharge may only be suggested by "reverse" zoning of minerals, such as increasing tetrahedral Al in hornblende (e.g. Bachmann and Dungan, 2002; Kiss et al., 2014), An content in plagioclase (e.g. Sliwinski et al., 2017), or Ti in quartz (e.g. Wark et al., 2007; Matthews et al., 2012).

During the maturation phase, one or more small reservoirs grow, coalesce and homogenize to form a large, unified magma reservoir (Fig. 7b, c, Table 1). At vents distributed over a given surface area, there is a transition from magmas of varied composition to magmas of a similar composition. At Long Valley caldera for example, there was a transition from three geochemical series of trachybasalts to dacites (the Central Sierran, the East Sierran and the Basin and Range from SW to NE) to a single geochemical series of rhyolites (Glass Mountain rhyolites) that became increasingly homogeneous with time (Fig. 3; Bailey, 2004; Hildreth, 2004). At Okataina, trace elements measured in zircons from the Kaharoa (0.7 ka), Whakatane (4.83 ka), and Te Rere (25 ka) eruptions record the same thermal and chemical pulse that followed the collapse of the Rotoiti caldera (61 ka) (Klemetti et al., 2011; Rubin et al., 2016). Vents from these eruptions are ~15 km apart, implying that there was a large interconnected magmatic system prior to the Rotoiti CCF eruption, and pockets of melt from this reservoir have survived for 10,000s of years. Hf isotopes in zircons from the Kaharoa, Waiohau (13.6 ka), Rerewhakaaitu (17.6 ka), and Okareka (21.9 ka) eruptions show a systematic change from rather homogeneous ratios before to more heterogeneous ratios after the Rotoiti CCF eruption (Fig. 6), highlighting the long term (>100 ky) zircon crystallization history from rather uniform melts that took place prior to caldera collapse (Storm et al., 2011; Rubin et al., 2016). Such examples of coalescing and homogenizing reservoirs have been observed at many other caldera systems, including one of the archetypical caldera-forming systems,

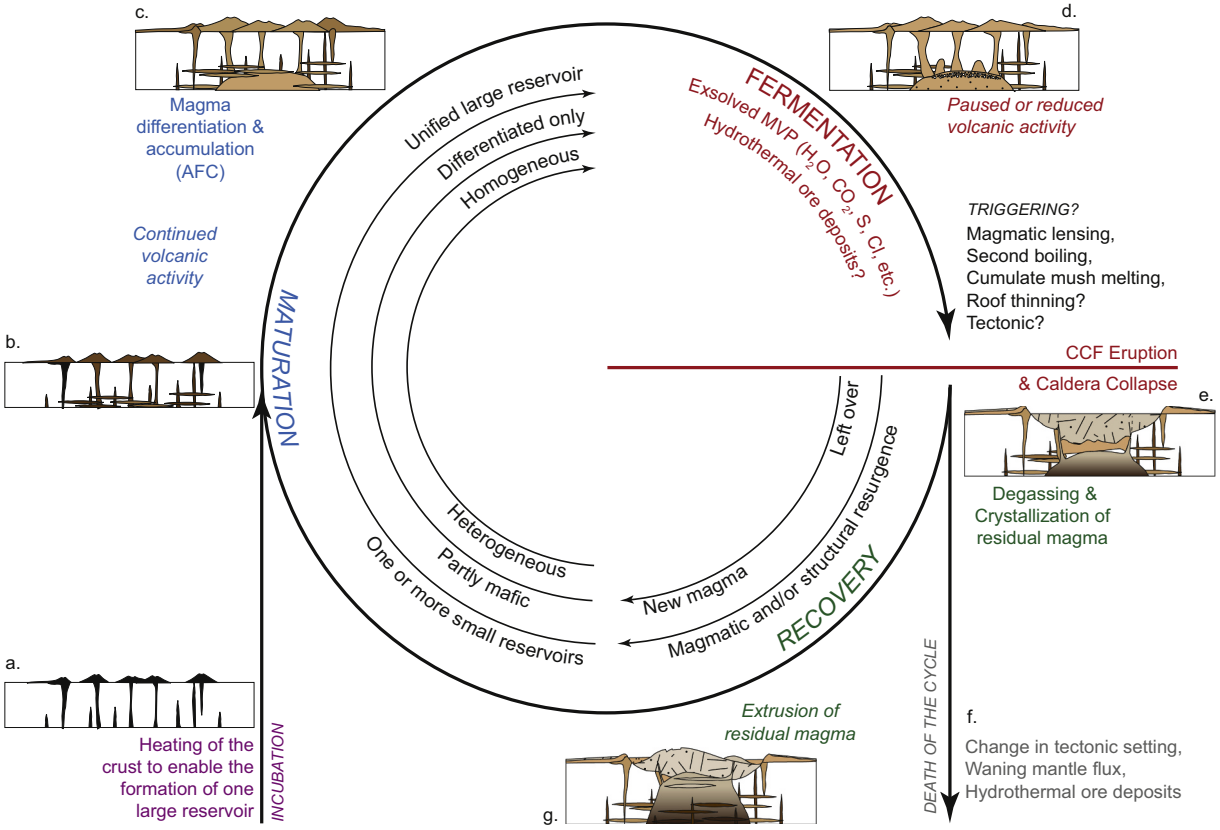

Fig. 7. Schematic representation of the caldera cycle. A monocyclic catastrophic caldera forming (CCF) volcanic system evolves from (a) a period of incubation, (b,c) a period of maturation (AFC – Assimilation and Fractional Crystallization), (d) a period of fermentation and intense production of a magmatic volatile phase (MVP), to (e) caldera collapse during a CCF eruption, and (f) the death of the cycle due to decreased magma influx from the lower crust or upper mantle. The temporal evolution of a polycyclic CCF system will be the same except that after the CCF eruption (e), a phase of recovery and active recharging (g) pushes the system to renewed maturation and the continuation of the cycle.

Yellowstone (Bindeman and Valley, 2001; Troch et al., 2017). This final reservoir can be a unique and homogeneous reservoir or can consist of an extensively interconnected network of reservoirs (Shane et al., 2005; Cole et al., 2014; Toba - Pearce et al., 2020). Local pressure and temperature conditions within the reservoir may however enable the development of small-scale heterogeneities within the melt, which can be recorded by the trace element compositions of minerals (e.g. zircons; Klemetti et al., 2011; Storm et al., 2011; pyroxenes; Ellis et al., 2014). It may also favor the development of vertical zoning in the melt composition and volatile content of the reservoir (e.g. Bishop Tuff - Hildreth, 1979; Wallace et al., 1999; Campi Flegrei - Forni et al., 2016, 2018).

For thermo-mechanical reasons, large volumes of magma are dominantly stored in a highly crystalline state (Marsh, 1981; Koyaguchi and Kaneko, 1999; Michaut and Jaupart, 2006; Huber et al., 2009; Gelman et al., 2013b; Cooper and Kent, 2014). This plays a key role in enabling the accumulation and differentiation of magmas. Highly crystalline magmas are beyond the rheological locking point, meaning that parts of the reservoir will be able to grow as they can no longer be tapped by eruptions. Continued replenishment prevents these parts of the reservoir from freezing completely (Bachmann and Bergantz, 2003; Michaut and Jaupart, 2006; Annen, 2009; Burgisser and Bergantz, 2011; Huber et al., 2011; Gelman et al., 2013b). The development of a crystal mush also provides an efficient mechanism to fractionate evolved melt from its solid counterpart, as crystal-liquid separation is the most effective around 50–70 vol% crystals (Bachmann and Bergantz, 2004; Dufek and Bachmann, 2010). After ~40–50% crystallization, magmas of andesitic to dacitic composition contain high-SiO_2 interstitial melt, which can become an eruptible high-silica rhyolite when it segregates from the mush (Bachmann and Bergantz, 2004). Magma accumulation and differentiation through the gradual development of an extensive crystal-mush might therefore be an essential step towards a CCF eruption.

Depending on the tectonic setting, magmas will differentiate by following different liquid lines of descent. Despite differences, most ignimbrites resulting from CCF eruptions can be explained by similar storage conditions (a crystalline mush) and chemical evolution (assimilation and fractional crystallization) (e.g. Fowler and Spera, 2010). Highly crystalline monotonous intermediate ignimbrites (e.g. Fish Canyon Tuff, Masonic Park Tuff, USA; Hildreth, 1981) and the Kos Plateau Tuff (Bachmann, 2010; Bachmann et al., 2012) correspond to the eruption of a remobilized crystal mush, whereas zoned ignimbrites, consisting mostly of crystal-poor high-silica rhyolites or the alkaline equivalents (e.g. Bishop Tuff (Hildreth, 2004; Evans et al., 2016), Campi Flegrei (Forni et al., 2016, 2018), Rabaul Pyroclastics (Fabbro et al., 2020), Matahina Ignimbrite (Deering et al., 2011b), Ammonia Tanks Tuff (Deering et al., 2011a) and Peach Spring Tuff in the USA (Foley et al., 2020)) correspond to the eruption of the crystal-poor cap that segregated from the mush (Huber et al., 2012). Typically, hydrous tectonic environments permit highly crystalline mushes to be remobilized by underplating mafic magmas and therefore both crystal-rich and crystal-poor magmas can erupt (Wolff et al., 2015). In contrast, in dry tectonic environments, highly crystalline mush cannot be efficiently remobilized by the underplating of mafic magmas and only crystal-poor magmas are erupted (Huber et al., 2010).

Some systems such as the Caetano caldera (Watts et al., 2016), the La Pacana Caldera System (Lindsay et al., 2001) and other caldera systems in the Altiplano-Puna Volcanic Complex (Kay et al., 2010) are believed to have formed largely by crustal anatexis based on their geochemistry and the abundance of xenoliths. Large degrees of crustal melting and

assimilation are thermally challenging to achieve and require a rather rare set of conditions (at least in convergent margin magmatism): hot mantle magmas (1350–1150 °C) and rather hot and fertile, ideally partially molten crustal rocks (Thompson et al., 2002 and references therein). These conditions may thus be more commonly found at the base of thickened continental crust, such as in the Altiplano-Puna Plateau (Kay et al., 2010). Based on thermal modelling, bulk crustal melting (and assimilation) takes place most pronouncedly at higher temperature and can be accompanied by fractionation of the resulting hybrid magma (Thompson et al., 2002; Dufek and Bergantz, 2005). If/when large scale crustal melting takes place, it will most likely occur at the beginning of the maturation phase, after incubation of the lower crust has primed the host rocks for melting (Dufek and Bergantz, 2005). The resulting hybrids will then follow a similar evolution as described above.

The volcanic activity associated with the maturation phase consists of distributed monogenetic vents or small volcanic edifices that are sometimes distributed along a nascent ring fracture and that erupt effusively and/or explosively (e.g. Glass Mountain Rhyolite in Long Valley, Kefalos domes in the Kos-Nisyros Volcanic Complex, the various dome complexes and pyroclastic sequences pre-Matahina and pre-Rotoiti ignimbrites (Fig. 1). Another compelling example is the Bearhead Rhyolite, a series of small-volume and mostly effusive silicic eruptions that represent the early phases of pre-collapse volcanism at the Valles caldera (Justet and Spell, 2001)). Recent numerical modelling of magma chamber growth during inter-CCF periods shows that magma reservoirs grow in a non-linear way (acceleration) at rates between $\sim 10^{-4}$ and 10^{-2} km^3/year, and evolve from a period of small but frequent eruptions to large and infrequent eruptions (Fig. 8; Townsend et al., 2019). This is associated with volatile accumulation in and gradual exsolution from the melt. For example, at Campi Flegrei, the dissolved water content is thought to increase from ~3 wt% post-Campanian Ignimbrite to ~6 wt% pre-Neapolitan Yellow Tuff (Fig. 4). At Rabaul, the dissolved water content increases from 1 to 2 wt% post-Memorial Ignimbrite to ~3 wt% pre-Rabaul Pyroclastics (Fig. 4). These trends mirror the compositional and temperature evolution of the system and reflect the physicochemical state of the reservoir. During the maturation phase we consider exsolved volatiles to be absent or transiently present from the reservoir, unlike later during the evolution of the system (Fig. 8).

3.3. Fermentation: extensive development of a magmatic volatile phase (MVP)

At the end of the maturation phase, the large reservoir likely contains a highly evolved, dominantly crystalline magma or mush that has generally reached volatile saturation, at least in the most crystalline parts at the edges of the system (Fig. 7d, Table 1). At magma reservoir pressures (~2 kb), this magmatic volatile phase (MVP) is likely in the form of a relatively saline supercritical fluid (e.g. Lowenstern, 2000). Such magmatic fluids were observed in quartz-hosted fluid inclusions of highly crystalline clasts in the Kos Plateau Tuff (Fiedrich et al., 2020), and by Transmission Electron Microscopy in biotites of the Kos Plateau Tuff (Bachmann, 2010). Similarly, constant Cl contents in quartz-hosted melt inclusions in Cerro Toledo Rhyolite and the Bishop Tuff (the latter also having halogen-rich biotites) require the presence and the partitioning of Cl into an MVP (Stix and Layne, 1996; Wallace et al., 1999). Experimentally determined pre-eruptive storage conditions for the Lower Pumice 1, Lower Pumice 2, Cape Riva, and Minoan CCF eruptions at Santorini (Greece) demonstrated that magmas were also saturated in a complex MVP (Cadoux et al., 2014). These examples show that silicic magmas erupted during CCF eruptions have significant amounts of exsolved MVP.

The exsolution of an MVP is a natural consequence of the continued differentiation of silicic magmas (Shinohara, 1994; Webster, 2004; Baker and Alletti, 2012). Crystallization increases the volatile content of melt (H_2O, CO_2, S, Cl, and other halogens), as volatiles are dominantly incompatible in the crystallizing phases. In addition, decreasing temperature and increasing silica content of the melt typically decreases the solubility (or partition coefficient) of these elements in the melt (Webster, 1997). While the pressure and Cl/H_2O ratio will control the type of magmatic volatile phase exsolved (i.e. vapor or magmatic

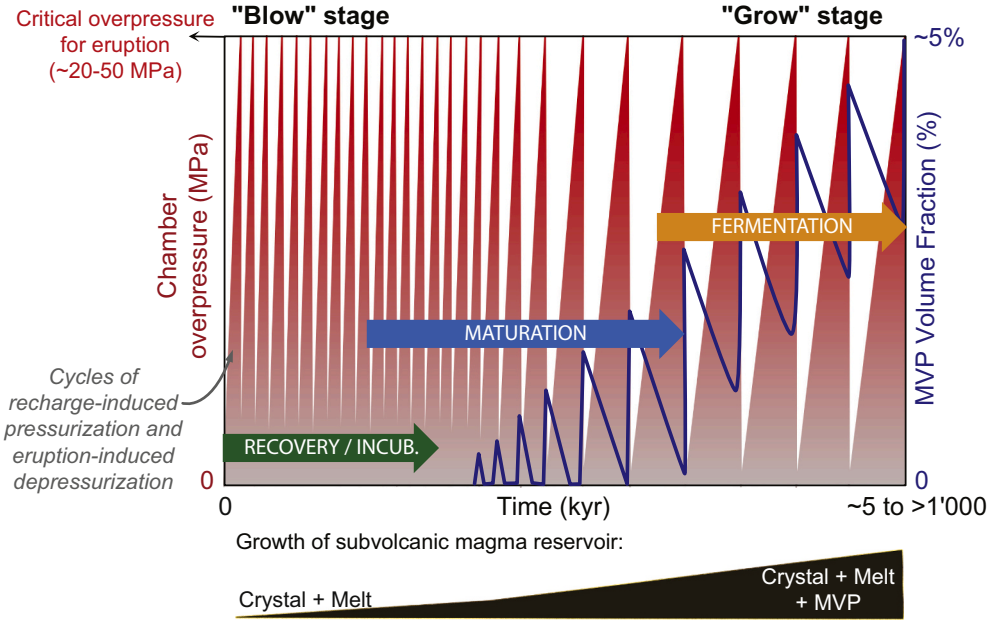

Fig. 8. Results from thermo-mechanical simulations tracking the evolution of pressure (red fields) and percentage of exsolved Magmatic Volatile Phase (MVP; blue line) in an open-system subvolcanic magma reservoir filled with a silicic magma undergoing constant recharge from below. Eruptions are triggered as the overpressure in the reservoir reaches a certain threshold (here considered to be between 20 and 50 MPa). Modified from Townsend et al. (2019). Green, blue and red arrows indicate the timings of the maturation, fermentation, and recovery/incubation phases, respectively, the duration of which will depend on the viscosity of the crust. Notice how the frequency of eruptions decreases with time, from an early "Blow" stage (frequent but small eruptions) to a later "Growth" stage (rare but voluminous eruptions). The transition from an initial incubation or recovery phase into the maturation phase will occur gradually when a reservoir starts to grow, and magmas are able to differentiate. At some point the magma reservoir is capable of hosting an exsolved MVP, which initially is fully expelled during an eruption but then gradually accumulates sufficiently to persist after an eruption. We propose that at this point the system transitions from the maturation to the fermentation phase. (For interpretation of the references to colour in this figure legend, the reader is referred to the web version of this article.)

hydrosaline fluids), the volatile abundance (mainly H_2O and CO_2) controls the timing of exsolution (Shinohara, 1994; Lowenstern, 2000; Webster, 2004). Hydrothermal activity is expected to be near or at its maximum during this period of the caldera cycle. The magma reservoir is at its largest and magmas are undergoing crystallization-induced volatile exsolution (i.e. second boiling). Volatiles in the crystal-rich regions of the reservoir will escape, possibly in pulses (Chelle-Michou et al., 2017) and combine with meteoric fluids heated by the particularly large sub-caldera reservoir. The surface expression would likely correspond to enhanced unrest in the form of ground motion (waxing and waning uplift and subsidence, also referred to as bradyseism) and diffuse degassing as observed at restless calderas like Campi Flegrei (e.g. Capaldi et al., 1992; Orsi et al., 1995; Chiodini et al., 2003; Aiuppa et al., 2013), Long Valley (Foulger et al., 2003; Hill, 2006; Hildreth, 2017) or Yellowstone (Lowenstern et al., 2006).

A part of the MVP phase will stay trapped in the melt-rich regions of the reservoir where bubbles are isolated and incapable of forming interconnected channels (Parmigiani et al., 2016, 2017). As a result, the compressibility of the mobile magma increases, making the reservoir harder to pressurize and thus decreasing the likelihood of eruptions (Degruyter and Huber, 2014; Townsend et al., 2019). The reservoir may then enter a phase of runaway growth (Karlstrom et al., 2010; Townsend et al., 2019) and continued magma differentiation. The onset of the fermentation phase could thus be viewed as the time from which an MVP phase is persistently present in the reservoir and no longer fully tapped by or consumed during eruptions (Fig. 8), as from this point in time the reservoir will become particularly and increasingly difficult to pressurize sufficiently to erupt. The frequency of eruptions largely decreases while their volume is expected to increase (Townsend et al., 2019).

Although the last known deposits are not necessarily the last deposits produced (these may have been obliterated from the geologic record during caldera collapse), observations of natural systems are in agreement with predictions from numerical modelling. At the Kos-Nisyros Volcanic Complex, ~150 ka elapsed between the eruption of the Cheri-Agios Mammas rhyolite dome and that of the Kos Plateau Tuff. At Okataina, there was a ~150 ky period of relative quiescence prior to the Rotoiti eruption (Cole et al., 2014). It thus seems that, particularly for larger systems, volcanic activity almost completely ceases as the reservoir grows during the fermentation phase (Stix and Layne, 1996; Degruyter et al., 2016). At Rabaul, titanomagnetites from the last known eruptions preceding the Memorial Ignimbrite and the Rabaul Pyroclastics have particularly high MnO contents, even higher than the titanomagnetites in the Memorial Ignimbrite and Rabaul Pyroclastics themselves (Fig. 5). This suggests that some pockets of melt experienced the largest degrees of cooling and melt differentiation during the fermentation phase. Similar features can be observed in the titanomagnetites from Campi Flegrei (Fig. 4). At Long Valley, the Rb/Sr ratio is particularly high in the melt of Glass Mountain rhyolites, higher than the most evolved melts in the Bishop Tuff, also potentially suggesting larger degrees of fractionation (Metz and Mahood, 1985, 1991; Davies and Halliday, 1998). Once these sub-caldera reservoirs enter such runaway growth conditions, one can only wonder what process is able to trigger an eruption?

3.4. Eruption triggering and catastrophic caldera collapse

Four main mechanisms of eruption triggering have been invoked for CCF eruptions: (1) over-pressurization of the reservoir by magma replenishment (Folch and Martí, 1998), volatile exsolution (Blake, 1984), and/or crystal mush remelting (Huber et al., 2011), (2) over-pressurization due to magma buoyancy (Caricchi et al., 2014; Malfait et al., 2014), (3) structural failure of the reservoir roof in response to prolonged heating and thinning (Gregg et al., 2012), and (4) external triggers (e.g. large earthquakes - Lindsay et al., 2001; Gottsmann et al., 2009; or rifting Allan et al., 2012). These mechanisms might be variably effective depending on the tectonic setting, dimensions of the reservoir, and petrologic properties of the magma (composition, crystallinity, volatile content), but they may also operate in conjunction, cumulatively increasing the over-pressurization of the reservoir until fracturing of the overlying rocks is achieved (Cañón-Tapia, 2014).

Magmas erupted during CCF eruptions are generally geochemically more diverse and reach less evolved compositions than those erupted immediately before the catastrophic event. Vertical gradients in magma crystallinity are also frequently observed. For example:

- The earliest erupted units of the Kos Plateau Tuff are crystal-poor while all subsequent units are crystal-rich (Allen, 2001). Gray andesitic and banded andesitic-and-rhyolitic pumices are rare but present in the upper stratigraphic units of the Kos Plateau Tuff (Allen, 2001). They have been attributed to magma recharge and associated mush reheating and remobilization (reduction in crystallinity), which is essential to enable the eruption of such a crystal-rich magma (Bachmann et al., 2019).
- Similarly, at Rabaul, mingled glass, rare mafic crystals and banded pumices are present at the top of the Rabaul Pyroclastics ignimbrite, and have been interpreted as signs of magma recharge trapped at the lower periphery of the reservoir (Fabbro et al., 2020). All ignimbrites at Rabaul are crystal-poor, and as their mineralogy consists exclusively of anhydrous phases (plagioclase, pyroxenes, titanomagnetite and apatite) mush melting and remobilization will be minimal.
- The Bishop Tuff has long been a typical example of vertically-zoned ignimbrite (Hildreth, 1979), with greater proportions of less-evolved pumice, more crystals (0.5–24 wt%) and higher Fe-Ti-oxide temperatures (up to ~820 °C) towards the top of the ignimbrite (base of the reservoir) (Hildreth and Wilson, 2007). This zoning has been attributed to gradual and incremental extraction of crystal-poor melt from the underlying mush system (Hildreth and Wilson, 2007), but also to the melting of this mush system in response to heating by recharging mafic to intermediate magmas (Wolff et al., 2015; Evans et al., 2016). This reheating and mush remobilization process is corroborated by incremental heating and Ar-Ar dating of Bishop Tuff sanidines, which reveals rapid pre-eruption remobilization from storage conditions close to solidus temperatures (Andersen et al., 2017).
- At Campi Flegrei, remarkable compositional and crystallinity variations (from phonolites with ~5% crystals at the bottom to trachytes with ~40% crystals at the top) are observed in the Campanian Ignimbrite (Forni et al., 2016) and strong evidence for mixing/mingling with a more mafic recharge magma and a cumulate melt are observed in the Neapolitan Yellow Tuff (Forni et al., 2018).
- At Okataina, the Rotoiti eruption has evidence for basalt emplaced on the floor of the rhyolitic reservoir, driving vigorous convection to produce the well-mixed dominant magma type (Shane et al., 2005), while the slightly compositionally-zoned crystal-poor Matahina ignimbrite has been shown to include, from its base to top, clasts from an extracted rhyolitic melt, the cumulate complement, and a recharging basalt (Deering et al., 2011b).

There are many other examples of mush rejuvenation (e.g. Ammomia Tanks Tuff (Deering et al., 2011a), Peach Spring Tuff (Foley et al., 2020), Fish Canyon Tuff (Bachmann et al., 2002)) including evidence for cognate cumulate mush melting (i.e. enrichment in Ba, Sr and Eu/Eu* and higher temperatures recorded by geothermometers towards the top of the sequence; Wolff et al., 2020). It is thus clear that, during a CCF eruption, evacuation of the crystal-poor, more evolved and more mobile magmas is often accompanied by the withdrawal of their crystal-rich roots, a process favored by the injection of more mafic and hotter recharge magmas conducive to mush remobilization.

Petrologic inspection of CCF-derived ignimbrites lends support to the first eruption triggering mechanism: over-pressurization of the reservoir by magma replenishment (Folch and Martí, 1998), volatile exsolution (Blake, 1984), and/or crystal mush remelting (Huber et al., 2011).

Significant overpressures are required to trigger an eruption from a large magma reservoir, as the surrounding crust behaves viscoelastically and can accommodate significant volume changes (Folch and Martí, 1998; Jellinek and DePaolo, 2003; Degruyter and Huber, 2014). A constant rate of magma replenishment is therefore not sufficient to reach the required overpressures, rather an increasing rate of magma replenishment is preferable (Degruyter and Huber, 2014). This can be potentially achieved by an increase in mantle flux or a focusing of ascending magmas towards the large reservoir through the modified stress field. Indeed, an overpressured reservoir will attract surrounding dykes that ascend from the mantle or lower crust (Muller et al., 2001; Karlstrom et al., 2009; Pansino and Taisne, 2019). The extensive development of a MVP by second boiling will also contribute to the pressurization of the system, and this may be supplemented by crystallization and volatile exsolution of the underplating replenishing mafic magmas (Francis et al., 1989; Folch and Martí, 1998; Stock et al., 2016). Lastly, additional overpressurization can be produced by partial remelting of the mush, as crystals are transformed into lower density melt, resulting in a volume increase (Huber et al., 2011). The catastrophic evacuation of a large reservoir may thus in fact be the direct and inevitable consequence of its runaway growth, favoring bubble accumulation, absorption of rising magmas over an ever-increasing capture radius, and melting of the deeper mush roots - all three processes cumulatively increasing the overpressurization of the reservoir. This situation, however, hinges on the (close to full) retention of the MVP in the growing reservoir. Any substantial leakage of the MVP would decrease the compressibility of the magma and the pressurization of the reservoir, most likely favoring magma storage in the crust (and the development of plutonic bodies).

The other eruption triggers (magma buoyancy, roof thinning, and external triggers) will leave little to no sign in the petrologic record and thus cannot be easily evaluated with the data presented here. They require some of the stored magma to be in an eruptible state, as they provide no mechanism for mush remobilization. Given the frequent to ubiquitous evidence for short-term reheating of caldera systems (whether crystal-rich or not) prior to a CCF eruption, it is likely that this process happens once a reservoir is large enough, no matter what the final trigger is. We expect all triggering processes to occur at the end of the Fermentation Phase (Fig. 7d, Table 1). However, if the trigger is tectonic (i.e. external) or roof collapse, the CCF eruption could possibly occur earlier, i.e. at the end of the Maturation Phase or early during the Fermentation Phase, if parts of the magma reservoir are in an eruptible state.

3.5. Continuation or death of the caldera cycle

During the climactic CCF eruption, most (if not all) of the mobile magma is evacuated from the reservoir (Karlstrom et al., 2012). The decompression that accompanies the CCF eruption leads to a significant degassing and crystallization wave in the left-over mush, leading to a substantial stiffening of the system (Bachmann et al., 2012). The type (piston, trapdoor, piecemeal, etc.) and extent of roof collapse during the CCF eruption influences the new reservoir geometry (Lipman, 2000; Cole et al., 2005). The system can go back to multiple, small, (partly) disconnected lenses of magma, or a single but significantly reduced, melt-poor reservoir (Fig. 7e, f, Table 1).

If the general conditions remain favorable through continued injections of magma from the mantle and lower crust at a sufficient rate to keep upper reservoirs viable (Karlstrom et al., 2010; Gelman et al., 2013b; Caricchi et al., 2014; Townsend et al., 2019; Townsend and Huber, 2020), the magma reservoir will gradually rebuild through a recovery phase, subsequent maturation and fermentation, until ultimately another CCF eruption occurs (Figs. 4–7). Conversely, the system will no longer be capable of producing CCF eruptions if (1) a large and shallow magma reservoir is no longer able to develop or (2) the residing crystal mush can no longer be rendered eruptible.

Some insights on the symptoms of a dying caldera system can be gleaned from the study of Eocene-Oligocene caldera systems, such as the Bonanza caldera in the Southern Rocky Mountain volcanic field, Colorado (Lipman et al., 2015) or the Caetano caldera in Nevada (Watts et al., 2016). A main issue, however, lies in the temporal resolution of these systems where the most precise dates come with errors of ±200 ky, which induces considerable uncertainty in the translation of these observations to modern systems. The preservation of the eruption record is also much less complete in these older systems, thus evidence for the detailed sequence of events pre- and post-CCF eruption might no longer exist. Nevertheless, it is interesting to note that most of the post-Caetano Tuff volcanic activity occurred shortly after the CCF eruption (Ar-Ar ages indistinguishable from the Caetano Tuff itself) and principally involved remnants of the roots of the shallow reservoir with the same composition as the upper Caetano Tuff (Watts et al., 2016). This suggests that no high-flux mafic magma recharge occurred post-CCF eruption. Similarly, post-Bonanza volcanic activity mostly occurred shortly after the CCF eruption (ages overlapping with those of the Bonanza Tuff) and spans the same range in composition as the very zoned Bonanza tuff itself (Lipman et al., 2015), with no signs of particularly high mafic recharge or cumulate melting. In both systems, cognate plutonic intrusions have been found to span a similar age range as the CCF eruption and post-CCF volcanic activity but do not extend younger. They are also quite evolved (Lipman et al., 2015; Watts et al., 2016). It is possible that the absence of signs of (abundant) recharge is key to determining the death of the caldera cycle. Detailed petrologic studies along the reconstructed stratigraphy of post-CCF deposits in such old systems would help constrain the characteristics of a waning caldera system.

3.6. Recovery: active recharging of the shallow reservoir

The structural uplift of the caldera floor shortly after collapse is termed “resurgence” (Smith and Bailey, 1968). It may occur at both monocyclic and polycyclic calderas. Structural resurgence corresponds to a readjustment of the rocks hosting the reservoir after it has been tapped (i.e. viscous rebound or regional detumescence; Marsh, 1984). Magmatic resurgence corresponds to a magmatic refilling of the shallowest parts of the reservoir, either by tapping slightly deeper parts of the system or due to renewed recharge from greater depths (e.g. Kennedy et al., 2012). During resurgence, magmas may or may not reach the surface, forming lava domes, flows, sills or laccoliths (e.g. Long Valley (Hildreth, 2004), Valles and Lake City calderas (Kennedy et al., 2012), Turkey Creek (du Bray and Pallister, 1999); Toba (de Silva et al., 2015; Mucek et al., 2017)).

At polycyclic calderas, the shallow reservoir recovers through active magma recharging and gradually evolves to the next CCF eruption. The recovery phase thus refers to any post-CCF activity involving the extrusion of magma at the surface with indications of magma recharge (Table 1). Erupted magmas are remobilized remnants of the large magma body, newly injected magmas from deeper in the system, or a mix of the two. When CCF magma remnants are too crystalline to be remobilized, the more mafic replenishing magmas (if present) are erupted directly. These will occasionally mix with pockets of remnant melt. The mafic products that erupt after a CCF event are (*i*) basaltic to andesitic as at the Kos-Nisyros Volcanic Complex (Fig. 2) and Rabaul (Fig. 5), (*ii*) trachybasaltic like at Campi Flegrei (Fig. 4), (*iii*) dacitic as at Okataina (Fig. 6; Shane and Smith, 2013) and Taupo (Gelman et al., 2013a; Barker et al., 2014), or even (*iv*) rhyolitic as at Long Valley (Fig. 3; Hildreth, 2004) but with clear signs of cumulate melting (i.e. sanidine and zircon resorption yielding crystal-free magmas with anomalously high Ba and Zr contents akin to cumulate melting signatures proposed for other systems; Wolff et al., 2020). These immediately post-CCF magmas are often hotter, dryer, and less oxidized than the CCF magma. For example, the first rhyodacites to rhyolites erupted from the Kos-Nisyros Volcanic Complex are up to >100 °C hotter than the Kos Plateau Tuff and pre-Kos Plateau Tuff rhyolites and their mineralogy tends to be more anhydrous (more plagioclase and less amphibole -

Fig. 2; Bachmann et al., 2012). Immediately post-CCF eruptions at Campi Flegrei and Rabaul record temperature increases of at least 100 °C (Figs. 4, 5). At Okataina, Fe-Ti oxides record an increase in temperature of >100 °C during the 10–15 ky following the Rotoiti eruption (Fig. 6). Immediately after the Oruanui CCF eruption at Taupo, the magma system also underwent heating and practically lacks any pre-Oruanui zircons (Gelman et al., 2013a; Barker et al., 2014). This is attributed to changes in the reservoir conditions following the CCF eruption.

Less evolved magmas will continue to reach the surface as long as a large, unified magma reservoir has not started to rebuild. It took ~40 ky at the Kos-Nisyros Volcanic Complex for rhyolitic magmas to reappear after the Kos Plateau Tuff eruption (Fig. 2), ~5 ky at Campi Flegrei for cold and more differentiated magmas to appear after the Neapolitan Yellow Tuff (Fig. 4), ~1.5 ky at Rabaul for dacitic magmas to reappear after the Memorial Ignimbrite and Rabaul Pyroclastics (Fig. 5), and 10–15 ky at Okataina before high-silica rhyolites were erupted following the Rotoiti eruption (Fig. 6). Although Hildreth (2004) considers that the Long Valley system is moribund, Flinders et al. (2018) have recently provided seismic evidence for abundant melt beneath the caldera depression. Interestingly, the lavas of the Northwest wall dacite chain (~30–40 ka) correspond to hybrid magmas that are the product of mixing between a trachydacite similar to that of Mammoth Mountain, a rhyolite similar to remnants of the Long Valley reservoir, and mafic enclaves (Bailey, 2004; Hildreth, 2004) and the mid-14th century Inyo eruption (which took place very close to the NW wall dacite chain) involved dacitic magma from the NW wall chain, rhyolite akin to the Mono domes magma, residual or thermally rejuvenated Long Valley magmatic mush, and andesitic enclaves (Hildreth, 2004 and references therein). This could suggest that a common reservoir has been forming over the past 30–40 ka at the confluence of these previously individualized systems, at the northwestern end of the low velocity anomaly imaged by Flinders et al. (2018).

It is challenging to strictly define the characteristics of the recovery phase, as each CCF eruption will have its own collapse dynamics and leave the reservoir in a different state; i.e. more or less emptied, more or less cooled and crystallized. Depending on the geometry and thermo-mechanical properties of the left-over reservoir, recovery may have different durations and leave a variably strong geochemical signature in the subsequently erupted magmas. We thus define the recovery phase as the period during which magmas show clear signs of thermal rejuvenation of the system, i.e. output of significantly/detectably more mafic magmas and/or geochemical signs of significant reheating and even melting of left-over material. Once the magma starts following differentiation trends somewhat akin to the pre-CCF situation, it is considered to have resumed a phase of maturation during which magmas evolve, volatiles start exsolving, and reservoirs grow. Because of the previously accumulated heat, the crust will remain viscoelastic for some time (a few hundred thousand years; Lipman, 2000). Therefore, the renewed growth of a large reservoir has the potential to be faster than for the first episode (no incubation phase is required).

The duration of a caldera cycle, from recovery, maturation, and fermentation to CCF eruption, depends on the volume of the reservoir, as is obvious from our case studies: Long Valley is the largest system and the slowest to evolve, while Rabaul is by far the smallest system and the quickest to evolve. However, within a given system, it is likely that recurring cycles change in duration as a function of the state of the emptied reservoir and the thermal regime of the surrounding crust (Degruyter et al., 2016; Townsend et al., 2019). For example, the duration of a caldera cycle changed from ~6.5 ka to ~3 ka pre- and post-Memorial Ignimbrite at Rabaul (Fig. 5), from ~225 ka to ~280 ka pre- and post-Matahina Ignimbrite at Okataina (Fig. 6), from 110 ka, to 49 ka, to ~18 ka between the oldest caldera collapse and the Minoan eruption at Santorini (Druitt and Francaviglia, 1992), and from 125 ka, to 18 ka, to 33 ka from the Aso-1 to Aso-4 caldera-forming eruptions at Aso caldera in Japan (Kaneko et al., 2007). The relative durations of the various phases (recovery versus maturation versus fermentation), however, may be expected to remain constant from one cycle to the next and from one system to the next, as they are essentially controlled by the thermo-mechanical evolution of the sub-caldera reservoir(s).

4. Application of the caldera cycle

At least 120 calderas have been restless in the past century, which corresponds to about half of the historically-active calderas known worldwide (Newhall and Dzurisin, 1988). However, not all episodes of unrest lead to an eruption and even less lead to a caldera-forming eruption (Acocella et al., 2015). Only a few (less than ten) silicic calderas are known to have formed in historical times, and these were small (≤10 km in diameter). In historical time, restlessness at a stratovolcano has culminated with an eruption nearly half of the time (Newhall and Dzurisin, 1988; Biggs et al., 2014). Similarly, about 40–50% of the time, unrest at silicic calderas leads to an eruption (typically explosive, generally VEI 1–3). On the other hand, restlessness at silicic calderas that have not erupted for 100 years or more results in an eruption 16% of the time. About 18% of the historic eruptions from all types of volcanoes worldwide occurred at calderas (Newhall and Dzurisin, 1988).

The caldera cycle is a concise framework that can be used to interpret geologic observations, unrest records, and petrologic data at a single caldera. If a restless caldera system has been placed in this framework, symptoms of unrest may be interpreted with more confidence with respect to the eruptive activity to be expected (or not). For example, we can now speculate that:

- The Kos-Nisyros Volcanic Complex is nearing the end of the maturation phase: Recently erupted magmas show signs of increased differentiation, decreased pre-eruptive temperatures and increased water contents (Fig. 4). Some parts of the reservoir (Yali rhyolites) are as cold, wet, oxidized, and differentiated as pre-Kos Plateau Tuff rhyolites, while other parts are not yet as evolved (Nisyros rhyolites). This suggests that a large reservoir has not fully amalgamated and homogenized yet (Bachmann et al., 2019). The low frequency of eruptions and intense activity of the hydrothermal system might suggest that the reservoir is starting a runaway growth phase in which an exsolved MVP is becoming increasingly present and important. Rare but potentially large-scale rhyolitic eruptions are to be expected in the geologically near future (like the most recent Nisyros and Yali products) and unrest will likely continue in response to the heightened hydrothermal activity.
- Long Valley is in the early maturation phase: Structural resurgence ended, remnants of the Long Valley/Bishop mush have been tapped, mafic magmas have reappeared and have started to differentiate (e.g. Mammoth Mountain), suggesting that the recovery phase is over. Small volumes of very differentiated rhyolitic magmas were erupted recently (i.e. Mono rhyolites) and there are possible signs of a coalescing reservoir at the confluence of the Long Valley caldera, Mammoth Mountain and Mono-Inyo systems. If mantle supply persists and the system progresses through the maturation phase, eruption frequency is expected to decrease while erupted volumes will increase. Ground deformation and unrest may increase and become similar to what is occurring in the Kos-Nisyros Volcanic Complex and Campi Flegrei, as the hydrothermal system grows and an MVP brews. The Long Valley system, however, is a very slowly evolving system and thus the maturation phase may last for ~1 Ma.
- Campi Flegrei is in the fermentation phase: The detailed stratigraphic reconstruction of the post-Neapolitan Yellow Tuff activity sheds light into the last ~15 ky of volcanic activity (Smith et al., 2011). The trends described by the intensive parameters are similar to those observed during the inter-caldera phase, with increased magma differentiation, a decrease in pre-eruptive temperatures and increase in water contents (Fig. 4). The frequency of eruption has also generally been decreasing. Petrological proxies coupled with

numerical modelling of magma chamber evolution suggest that the magmatic system is currently saturated in volatiles (Forni et al., 2018) and is thus undergoing a period of runaway growth. Unrest and bradiseismic activity is likely to continue as the system brews. Although infrequent, more "Monte Nuovo-like" eruptions can be expected to occur.

- Rabaul is in the mid-maturation phase: A dacitic magma reservoir is currently present but is frequently replenished by basalts (Bouvet de Maisonneuve et al., 2015), suggesting that the reservoir isn't fully developed yet and capable of blocking magma recharge in its periphery (Fabbro et al., 2020). Unfortunately, the recovery phase is not preserved in the geologic record, thus the evolution of the system cannot be traced in detail. There are signs of the transient presence of an MVP in the reservoir, particularly associated with explosive eruptions (Bernard and Bouvet de Maisonneuve, 2020), hinting to a system in the late stages of the maturation phase. As for the Kos-Nisyros Volcanic Complex, the level of unrest may be expected to increase, eruption frequency will decrease while their volume will increase, as the reservoir grows and gradually accumulates an MVP.
- Okataina is in the early to mid-maturation phase: Based on trends in bulk rock composition and pre-eruptive temperatures (Fig. 6), the recovery phase would be over. However, more information about the reservoir homogeneity, size, and presence of an MVP would be needed to fully assess the current status of the system.

It seems likely that another CCF eruption might occur from most (if not all) of the present case studies in a geologically near future. Although this near future may correspond to a thousand (Rabaul) or even a million (Long Valley) years, inter-CCF activity can still be violently explosive and poses a threat to the local communities, particularly when the system reaches the fermentation phase. Individual eruptions between collapse cycles are at least one order of magnitude less voluminous ($\leq$1–10 km^3). However, small eruptions for these systems can still represent large eruptions for our human society (i.e. VEI $\geq$ 6; Pinatubo-like eruptions).

We suggest placing calderas worldwide within this framework in order to better understand the steps and phases of a caldera cycle and their durations, as well as what the global, regional, tectonic and magmatic controls on these cycles are. The duration of a cycle and the volume of accumulated and erupted magma are likely a function of the tectonic setting (convergence rate, obliquity, slab age, magma production rate, etc.) but many of these relationships need to be inspected further. Global studies have explored the control of such geodynamic parameters on the occurrence and distribution of calderas (Hughes and Mahood, 2008; Sheldrake et al., 2020) but the correlations are mostly weak. If the size and thermomechanical requirements of these systems are taken into account, the rational for small and fast recurring CCF eruptions like at Rabaul versus large and infrequent CCF eruptions like at Yellowstone or Toba may be uncovered. With more studies focusing on the reconstruction of caldera cycles, we could (1) test the robustness of the proposed framework, (2) evaluate whether the relative durations of the various phases are similar during successive CCF eruptions and among systems, and (3) refine the petrologic, geophysical, and unrest characteristics of the state of a system. This will help to find clues about where to expect the next CCF-eruption.

Declaration of Competing Interest

The authors declare that they have no known competing financial interests or personal relationships that could have appeared to influence the work reported in this paper.

Acknowledgements

The authors thank an anonymous reviewer and the editor for their comments and manuscript handling. The authors wish to acknowledge the constructive comments of P. Lipman on a first version of this manuscript. This work was supported by the Earth Observatory of Singapore (contribution no. 373) via its funding from the National Research Foundation Singapore and the Singapore Ministry of Education under the Research Centres of Excellence initiative, as well as by the National Research Foundation of Singapore, grant NRF-NRFF2016-04. OB received funding from the Swiss National Science Foundation, grant number 200021_178928.

References

Acocella, V., Di Lorenzo, R., Newhall, C.G., Scandone, R., 2015. An overview of recent (1988 to 2014) caldera unrest: knowledge and perspectives. Rev. Geophys. 53, 896–955. https://doi.org/10.1002/2015RG000492.

Aiuppa, A., Tamburello, G., Di Napoli, R., Cardellini, C., Chiodini, G., Giudice, G., Grassa, F., Pedone, M., 2013. First observations of the fumarolic gas output from a restless caldera: implications for the current period of unrest (2005–2013) at Campi Flegrei. Geochem. Geophys. Geosyst. 14, 4153–4169. https://doi.org/10.1002/ggge.20261.

Albert, P.G., Giaccio, B., Isaia, R., Costa, A., Niespolo, E.M., Nomade, S., Pereira, A., Renne, P.R., Hinchliffe, A., Mark, D.F., Brown, R.J., Smith, V.C., 2019. Evidence for a large-magnitude eruption from Campi Flegrei caldera (Italy) at 29 ka. Geology 47, 595–599. https://doi.org/10.1130/G45805.1.

Allan, A.S.R., Wilson, C.J.N., Millet, M.A., Wysoczanski, R.J., 2012. The invisible hand: tectonic triggering and modulation of a rhyolitic supereruption. Geology 40, 563–566. https://doi.org/10.1130/G32969.1.

Allen, S.R., 2001. Reconstruction of a major caldera-forming eruption from pyroclastic deposit characteristics: Kos Plateau Tuff, eastern Aegean Sea. J. Volcanol. Geotherm. Res. 105, 141–162. https://doi.org/10.1016/S0377-0273(00)00222-5.

Andersen, N.L., Jicha, B.R., Singer, B.S., Hildreth, W., 2017. Incremental heating of Bishop Tuff sanidine reveals preeruptive radiogenic Ar and rapid remobilization from cold storage. Proc. Natl. Acad. Sci. U. S. A. 114, 12407–12412. https://doi.org/10.1073/pnas.1709581114.

Annen, C., 2009. From plutons to magma chambers: thermal constraints on the accumulation of eruptible silicic magma in the upper crust. Earth Planet. Sci. Lett. 284, 409–416. https://doi.org/10.1016/j.epsl.2009.05.006.

Bachmann, O., 2010. The petrologic evolution and pre-eruptive conditions of the rhyolitic Kos Plateau Tuff (Aegean arc). Cent. Eur. J. Geosci. 2, 270–305. https://doi.org/10.2478/v10085-010-0009-4.

Bachmann, O., Bergantz, G.W., 2003. Rejuvenation of the Fish Canyon magma body: a window into the evolution of large-volume silicic magma systems. Geology 31, 789–792. https://doi.org/10.1130/G19764.1.

Bachmann, O., Bergantz, G.W., 2004. On the origin of crystal-poor rhyolites: extracted from batholithic crystal mushes. J. Petrol. 45, 1565–1582. https://doi.org/10.1093/petrology/egh019.

Bachmann, O., Dungan, M.A., 2002. Temperature-induced Al-zoning in hornblendes of the Fish Canyon magma, Colorado. Am. Mineral. 87, 1062–1076. https://doi.org/10.2138/am-2002-8-903.

Bachmann, O., Dungan, M.A., Lipman, P.W., 2002. The Fish Canyon magma body, San Juan Volcanic Field, Colorado: rejuvenation and eruption of an upper-crustal Batholith. J. Petrol. 43, 1469–1503. https://doi.org/10.1093/petrology/43.8.1469.

Bachmann, O., Charlier, B.L.A., Lowenstern, J.B., 2007. Zircon crytallization and recycling in the magma chamber of the rhyolitic Kos Plateau Tuff (Aegean arc). Geology 35, 73–76. https://doi.org/10.1130/G23151A.1.

Bachmann, O., Schoene, B., Schnyder, C., Spikings, R., 2010. The 40 Ar/ 39 Ar and U/Pb dating of young rhyolites in the Kos-Nisyros volcanic complex, Eastern Aegean Arc, Greece: age discordance due to excess 40 Ar in biotite. Geochem. Geophys. Geosyst. 11 https://doi.org/10.1029/2010gc003073 n/a-n/a.

Bachmann, O., Deering, C.D., Ruprecht, J.S., Huber, C., Skopelitis, A., Schnyder, C., 2012. Evolution of silicic magmas in the Kos-Nisyros volcanic center, Greece: a petrological cycle associated with caldera collapse. Contrib. Mineral. Petrol. 163, 151–166. https://doi.org/10.1007/s00410-011-0663-y.

Bachmann, O., Allen, S.R., Bouvet de Maisonneuve, C., 2019. The Kos–Nisyros–Yali volcanic field. Elements 15, 191–196. https://doi.org/10.2138/gselements.15.3.191.

Bacon, C.R., 1983. Eruptive history of Mount Mazama and Crater Lake Caldera, Cascade Range, USA. J. Volcanol. Geotherm. Res. 18, 57–115. https://doi.org/10.1016/0377-0273(83)90004-5.

Bailey, R.A., 2004. Eruptive history and chemical evolution of the precaldera and postcaldera basalt-dacite sequences, Long Valley, California: implications for magma sources, current seismic unrest, and future volcanism. US Geol. Surv. Prof. Pap. 1–75. https://doi.org/10.3133/pp1692.

Baker, D.R., Alletti, M., 2012. Fluid saturation and volatile partitioning between melts and hydrous fluids in crustal magmatic systems: the contribution of experimental measurements and solubility models. Earth Sci. Rev. 114, 298–324. https://doi.org/10.1016/j.earscirev.2012.06.005.

Barker, S.J., Wilson, C.J.N., Smith, E.G.C., Charlier, B.L.A., Wooden, J.L., Hiess, J., Ireland, T.R., 2014. Post-supereruption magmatic reconstruction of Taupo volcano (New Zealand), as reflected in zircon ages and trace elements. J. Petrol. 55, 1511–1533.

Bernard, O., Bouvet de Maisonneuve, C., 2020. Controls on eruption style at Rabaul, Papua New Guinea – insights from microlites, porosity and permeability

measurements. J. Volcanol. Geotherm. Res. 406, 107068. https://doi.org/10.1016/j.jvolgeores.2020.107068.
Biggs, J., Ebmeier, S.K., Aspinall, W.P., Lu, Z., Pritchard, M.E., Sparks, R.S.J., Mather, T. A., 2014. Global link between deformation and volcanic eruption quantified by satellite imagery. Nat. Commun. 5 https://doi.org/10.1038/ncomms4471.
Bindeman, I.N., Valley, J.W., 2001. Low-δ18O rhyolites from Yellowstone: magmatic evolution based on analyses of zircons and individual phenocrysts. J. Petrol. 42, 1491–1517.
Blake, S., 1984. Volatile oversaturation during the evolution of silicic magma chambers as an eruption trigger. J. Geophys. Res. 89, 8237–8244.
Bouvet de Maisonneuve, C., Costa, F., Patia, H., Huber, C., 2015. Mafic magma replenishment, unrest and eruption in a caldera setting: insights from the 2006 eruption of Rabaul (Papua New Guinea). Geol. Soc. Spec. Publ. 422, 17–39. https://doi.org/10.1144/SP422.2.
Braschi, E., Francalanci, L., Vougioukalakis, G.E., 2012. Inverse differentiation pathway by multiple mafic magma refilling in the last magmatic activity of Nisyros Volcano, Greece. Bull. Volcanol. 74, 1083–1100. https://doi.org/10.1007/s00445-012-0585-1.
Braschi, E., Francalanci, L., Tommasini, S., Vougioukalakis, G.E., 2014. Unraveling the hidden origin and migration of plagioclase phenocrysts by in situ Sr isotopes: the case of final dome activity at Nisyros volcano, Greece. Contrib. Mineral. Petrol. 167, 1–25. https://doi.org/10.1007/s00410-014-0988-4.
Buettner, A., Kleinhanns, I.C., Rufer, D., Hunziker, J.C., Villa, I.M., 2005. Magma generation at the easternmost section of the Hellenic arc: Hf, Nd, Pb and Sr isotope geochemistry of Nisyros and Yali volcanoes (Greece). Lithos 83, 29–46. https://doi.org/10.1016/j.lithos.2005.01.001.
Burgisser, A., Bergantz, G.W., 2011. A rapid mechanism to remobilize and homogenize highly crystalline magma bodies. Nature 471, 212–217. https://doi.org/10.1038/nature09799.
Bursik, M., Sieh, K., Meltzner, A., 2014. Deposits of the most recent eruption in the Southern Mono Craters, California: description, interpretation and implications for regional marker tephras. J. Volcanol. Geotherm. Res. 275, 114–131. https://doi.org/10.1016/j.jvolgeores.2014.02.015.
Cadoux, A., Scaillet, B., Druitt, T.H., Deloule, E., 2014. Magma storage conditions of large plinian eruptions of santorini volcano (Greece). J. Petrol. 55, 1129–1171. https://doi.org/10.1093/petrology/egu021.
Cañón-Tapia, E., 2014. Volcanic eruption triggers: a hierarchical classification. Earth Sci. Rev. 129, 100–119. https://doi.org/10.1016/j.earscirev.2013.11.011.
Capaldi, G., Pece, R., Veltri, C., 1992. Radon variation in groundwaters in the Campi Flegrei Caldera (southern Italy) during and after the 1982–1984 bradyseismic crisis. Pure Appl. Geophys. 138, 77–93.
Caricchi, L., Annen, C., Blundy, J., Simpson, G., Pinel, V., 2014. Frequency and magnitude of volcanic eruptions controlled by magma injection and buoyancy. Nat. Geosci. 7, 126–130. https://doi.org/10.1038/ngeo2041.
Chelle-Michou, C., Rottier, B., Caricchi, L., Simpson, G., 2017. Tempo of magma degassing and the genesis of porphyry copper deposits. Sci. Rep. 7, 1–12. https://doi.org/10.1038/srep40566.
Chesner, C.A., Rose, W.I., 1991. Stratigraphy of the Toba Tuffs and the evolution of the Toba Caldera Complex, Sumatra, Indonesia. Bull. Volcanol. 53, 343–356. https://doi.org/10.1007/BF00280226.
Chesner, C., Rose, W.I., Deino, A.L., Drake, R., Westgate, J.A., 1991. Eruptive history of Earth's largest Quaternary caldera (Toba, Indonesia) clarified. Geology 19, 200–203.
Chiodini, G., Todesco, M., Caliro, S., Del Gaudio, C., Macedonio, G., Russo, M., 2003. Magma degassing as a trigger of bradyseismic events: the case of Phlegrean Fields (Italy). Geophys. Res. Lett. 30, 1–4. https://doi.org/10.1029/2002GL016790.
Chiodini, G., Paonita, A., Aiuppa, A., Costa, A., Caliro, S., De Martino, P., Acocella, V., Vandemeulebrouck, J., 2016. Magmas near the critical degassing pressure drive volcanic unrest towards a critical state. Nat. Commun. 7, 1–9.
Christiansen, R.L., 2001. The Quaternary and Pliocene Yellowstone Plateau volcanic field of Wyoming, Idaho, and Montana. US Geol. Surv. Prof. Pap. 729. https://doi.org/10.3133/pp729G.
Cole, J.W., 1990. Structural control and origin of volcanism in the Taupo volcanic zone, New Zealand. Bull. Volcanol. 52, 445–459.
Cole, J.W., Milner, D.M., Spinks, K.D., 2005. Calderas and caldera structures: a review. Earth Sci. Rev. 69, 1–26. https://doi.org/10.1016/j.earscirev.2004.06.004.
Cole, J.W., Spinks, K.D., Deering, C.D., Nairn, I.A., Leonard, G.S., 2010. Volcanic and structural evolution of the Okataina Volcanic Centre; dominantly silicic volcanism associated with the Taupo Rift, New Zealand. J. Volcanol. Geotherm. Res. 190, 123–135. https://doi.org/10.1016/j.jvolgeores.2009.08.011.
Cole, J.W., Deering, C.D., Burt, R.M., Sewell, S., Shane, P.A.R., Matthews, N.E., 2014. Okataina Volcanic Centre, Taupo Volcanic Zone, New Zealand: a review of volcanism and synchronous pluton development in an active, dominantly silicic caldera system. Earth Sci. Rev. 128, 1–17. https://doi.org/10.1016/j.earscirev.2013.10.008.
Cooper, K.M., Kent, A.J.R., 2014. Rapid remobilization of magmatic crystals kept in cold storage. Nature 506, 480–483. https://doi.org/10.1038/nature12991.
Dabalakis, P., Vougioukalakis, G., 1993. The Kefalos Tuff Ring (W. Kos): depositional mechanisms, vent position and model of the evolution of the eruptive activity. Bull. Geol. Soc. Greece 28, 259–273.
Danišík, M., Shane, P., Schmitt, A.K., Hogg, A., Santos, G.M., Storm, S., Evans, N.J., Keith Fifield, L., Lindsay, J.M., 2012. Re-anchoring the late Pleistocene tephrochronology of New Zealand based on concordant radiocarbon ages and combined 238U/ 230Th disequilibrium and (U-Th)/He zircon ages. Earth Planet. Sci. Lett. 349–350, 240–250. https://doi.org/10.1016/j.epsl.2012.06.041.
Davies, G.R., Halliday, A.N., 1998. Development of the Long Valley rhyolitic magma system: strontium and neodymium isotope evidence from glasses and individual phenocrysts. Geochim. Cosmochim. Acta 62, 3561–3574. https://doi.org/10.1016/s0016-7037(98)00247-6.
de Silva, S.L., Gosnold, W.D., 2007. Episodic construction of batholiths: insights from the spatiotemporal development of an ignimbrite flare-up. J. Volcanol. Geotherm. Res. 167, 320–335. https://doi.org/10.1016/j.jvolgeores.2007.07.015.
de Silva, S.L., Gregg, P.M., 2014. Thermomechanical feedbacks in magmatic systems: implications for growth, longevity, and evolution of large caldera-forming magma reservoirs and their supereruptions. J. Volcanol. Geotherm. Res. 282, 77–91. https://doi.org/10.1016/j.jvolgeores.2014.06.001.
de Silva, S.L., Mucek, A.E., Gregg, P.M., Pratomo, I., 2015. Resurgent Toba - field, chronologic, and model constraints on time scales and mechanisms of resurgence at large calderas. Front. Earth Sci. 3 https://doi.org/10.3389/feart.2015.00025.
Deering, C.D., 2009. Cannibalization of an amphibole-rich andesitic progenitor induced by caldera-collapse during the Matahina eruption: evidence from amphibole compositions. Am. Mineral. 94, 1162–1174. https://doi.org/10.2138/am.2009.3135.
Deering, C.D., Bachmann, O., Vogel, T.A., 2011a. The Ammonia Tanks Tuff: erupting a melt-rich rhyolite cap and its remobilized crystal cumulate. Earth Planet. Sci. Lett. 310, 518–525. https://doi.org/10.1016/j.epsl.2011.08.032.
Deering, C.D., Cole, J.W., Vogel, T.A., 2011b. Extraction of crystal-poor rhyolite from a hornblende-bearing intermediate mush: a case study of the caldera-forming Matahina eruption, Okataina volcanic complex. Contrib. Mineral. Petrol. 161, 129–151. https://doi.org/10.1007/s00410-010-0524-0.
Degruyter, W., Huber, C., 2014. A model for eruption frequency of upper crustal silicic magma chambers. Earth Planet. Sci. Lett. 403, 117–130. https://doi.org/10.1016/j.epsl.2014.06.047.
Degruyter, W., Huber, C., Bachmann, O., Cooper, K.M., Kent, A.J.R., 2016. Magma reservoir response to transient recharge events: the case of Santorini volcano (Greece). Geology 44, 23–26. https://doi.org/10.1130/G37333.1.
Deino, A.L., Orsi, G., de Vita, S., Piochi, M., 2004. The age of the Neapolitan Yellow Tuff caldera-forming eruption (Campi Flegrei caldera–Italy) assessed by 40Ar/39Ar dating method. J. Volcanol. Geotherm. Res. 133, 157–170.
Di Paola, G.M., 1974. Volcanology and petrology of Nisyros Island (Dodecanese, Greece). Bull. Volcanol. 38, 944–987. https://doi.org/10.1007/BF02597100.
Di Vito, M., Lirer, L., Mastrolorenzo, G., Rolandi, G., 1987. The 1538 Monte Nuovo eruption (Campi Flegrei, Italy). Bull. Volcanol. 49, 608–615.
Dietrich, V.J., Lagios, E., 2018. Nisyros Volcano. Active Vol. ed.. Springer. https://doi.org/10.1007/978-3-319-55460-0 ISSN.
Dietrich, V.J., Popa, R.-G., 2018. Petrology and geochemistry of lavas and pyroclastics. In: Nisyros Volcano. Springer, pp. 103–144.
Druitt, T.H., Francaviglia, V., 1992. Caldera formation on Santorini and the physiography of the islands in the late Bronze Age. Bull. Volcanol. 54, 484–493.
du Bray, E.A., Pallister, J.S., 1999. Recrystallization and anatexis along the plutonic-volcanic contact of the Turkey Creek caldera, Arizona. Geol. Soc. Am. Bull. 111, 143–153.
Dufek, J., Bachmann, O., 2010. Quantum magmatism: magmatic compositional gaps generated by melt-crystal dynamics. Geology 38, 687–690. https://doi.org/10.1130/G30831.1.
Dufek, J., Bergantz, G.W., 2005. Lower crustal magma genesis and preservation: a stochastic framework for the evaluation of basalt-crust interaction. J. Petrol. 46, 2167–2195. https://doi.org/10.1093/petrology/egi049.
Ellis, B.S., Bachmann, O., Wolff, J.A., 2014. Cumulate fragments in silicic ignimbrites: the case of the Snake River Plain. Geology 42, 431–434. https://doi.org/10.1130/G35399.1.
Evans, B.W., Hildreth, W., Bachmann, O., Scaillet, B., 2016. In defense of magnetite-ilmenite thermometry in the Bishop Tuff and its implication for gradients in silicic magma reservoirs. Am. Mineral. 101, 469–482. https://doi.org/10.2138/am-2016-5367.
Fabbro, G.N., McKee, C.O., Sindang, M.E., Eggins, S., Bouvet de Maisonneuve, C., 2020. Variable mafic recharge across a caldera cycle at Rabaul, Papua New Guinea. J. Volcanol. Geotherm. Res. 393, 106810. https://doi.org/10.1016/j.jvolgeores.2020.106810.
Fiedrich, A.M., Laurent, O., Heinrich, C.A., Bachmann, O., 2020. Melt and fluid evolution in an upper-crustal magma reservoir, preserved by inclusions in juvenile clasts from the Kos Plateau Tuff, Aegean Arc, Greece. Geochim. Cosmochim. Acta 280, 237–262. https://doi.org/10.1016/j.gca.2020.03.038.
Flinders, A.F., Shelly, D.R., Dawson, P.B., Hill, D.P., Tripoli, B., Shen, Y., 2018. Seismic evidence for significant melt beneath the Long Valley Caldera, California, USA. Geology 46, 799–802. https://doi.org/10.1130/G45094.1.
Flude, S., Storey, M., 2016. 40Ar/39Ar age of the Rotoiti Breccia and Rotoehu Ash, Okataina Volcanic Complex, New Zealand, and identification of heterogeneously distributed excess 40Ar in supercooled crystals. Quat. Geochronol. 33, 13–23. https://doi.org/10.1016/j.quageo.2016.01.002.
Folch, A., Martí, J., 1998. The generation of overpressure in felsic magma chambers by replenishment. Earth Planet. Sci. Lett. 163, 301–314. https://doi.org/10.1016/S0012-821X(98)00196-4.
Foley, M.L., Miller, C.F., Gualda, G.A.R., 2020. Architecture of a super-sized magma chamber and remobilization of its basal cumulate (Peach Spring Tuff, USA). J. Petrol. 61 (1), egaa020. https://doi.org/10.1093/petrology/egaa020.
Forni, F., Bachmann, O., Mollo, S., De Astis, G., Gelman, S.E., Ellis, B.S., 2016. The origin of a zoned ignimbrite: insights into the Campanian Ignimbrite magma chamber (Campi Flegrei, Italy). Earth Planet. Sci. Lett. 449, 259–271. https://doi.org/10.1016/j.epsl.2016.06.003.
Forni, F., Degruyter, W., Bachmann, O., De Astis, G., Mollo, S., 2018. Long-Term magmatic evolution reveals the beginning of a new caldera cycle at Campi Flegrei. Sci. Adv. 4 https://doi.org/10.1126/sciadv.aat9401.

Foulger, G.R., Julian, B.R., Pitt, A.M., Hill, D.P., Malin, P.E., Shalev, E., 2003. Three-dimensional crustal structure of Long Valley caldera, California, and evidence for the migration of CO2 under Mammoth Mountain. J. Geophys. Res. Solid Earth 108, 1–16. https://doi.org/10.1029/2000jb000041.

Fowler, S.J., Spera, F.J., 2010. A metamodel for crustal magmatism: phase equilibria of giant ignimbrites. J. Petrol. 51, 1783–1830. https://doi.org/10.1093/petrology/egq039.

Francalanci, L., Varekamp, J.C., Vougioukalakis, G.E., Innocenti, F., Manetti, P., 2007. Is there a compositional gap at Nisyros volcano? A comment on: magma generation at the easternmost section of the Hellenic arc: Hf, Nd, Pb and Sr isotope geochemistry of Nisyros and Yali volcanoes (Greece) [Lithos 83 (2005) 29-46]. Lithos 95, 458–461. https://doi.org/10.1016/j.lithos.2006.06.016.

Francis, P.W., Sparks, R.S.J., Hawkesworth, C.J., Thorpe, R.S., Pyle, D.M., Tait, S.R., Mantovani, M.S., McDermott, F., 1989. Petrology and geochemistry of volcanic rocks of the Cerro Galan caldera, rt Argentina. Geol. Mag. 126, 515–547.

Fytikas, M., Giuliani, O., Innocenti, F., Marinelli, G.T., Mazzuoli, R., 1976. Geochronological data on recent magmatism of the Aegean Sea. Tectonophysics 31, T29–T34.

Gelman, S.E., Deering, C.D., Gutierrez, F.J., Bachmann, O., 2013a. Evolution of the Taupo Volcanic Center, New Zealand: petrological and thermal constraints from the Omega dacite. Contrib. Mineral. Petrol. 166, 1355–1374. https://doi.org/10.1007/s00410-013-0932-z.

Gelman, S.E., Gutiérrez, F.J., Bachmann, O., 2013b. On the longevity of large upper crustal silicic magma reservoirs. Geology 41, 759–762. https://doi.org/10.1130/G34241.1.

Giaccio, B., Hajdas, I., Isaia, R., Deino, A., Nomade, S., 2017. High-precision 14 C and 40 Ar/39 Ar dating of the Campanian Ignimbrite (Y-5) reconciles the time-scales of climatic-cultural processes at 40 ka. Sci. Rep. 7, 1–10.

Gottsmann, J., Lavallée, Y., Martí, J., Aguirre-Díaz, G., 2009. Magma-tectonic interaction and the eruption of silicic batholiths. Earth Planet. Sci. Lett. 284, 426–434. https://doi.org/10.1016/j.epsl.2009.05.008.

Gregg, P.M., De Silva, S.L., Grosfils, E.B., Parmigiani, J.P., 2012. Catastrophic caldera-forming eruptions: thermomechanics and implications for eruption triggering and maximum caldera dimensions on Earth. J. Volcanol. Geotherm. Res. 241–242, 1–12. https://doi.org/10.1016/j.jvolgeores.2012.06.009.

Groceix, M.H., 1873. Sur l'état du volcan de Nisyros au mois de mars 1873. Compte Rendu. Séances Acad. Sci. Paris LXXVII 597–601.

Guillong, M., Von Quadt, A., Sakata, S., Peytcheva, I., Bachmann, O., 2014. LA-ICP-MS Pb-U dating of young zircons from the Kos-Nisyros volcanic centre, SE Aegean arc. J. Anal. At. Spectrom. 29, 963–970. https://doi.org/10.1039/c4ja00009a.

Heumann, A., Davies, G.R., 1997. Isotopic and chemical evolution of the post-caldera rhyolitic system at Long Valley, California. J. Petrol. 38 (12), 1661–1678. https://doi.org/10.1093/petroj/38.12.1661.

Hildreth, W., 1979. The Bishop Tuff: Evidence for the Origin of Compositional Zonation in Silicic Magma Chambers d, pp. 43–76. https://doi.org/10.1130/spe180-p43.

Hildreth, W., 1981. Gradients in silicic magma chambers. J. Geophys. Res. 86 (B11), 10153–10192.

Hildreth, W., 2004. Volcanological perspectives on Long Valley, Mammoth Mountain, and Mono Craters: several contiguous but discrete systems. J. Volcanol. Geotherm. Res. 136, 169–198. https://doi.org/10.1016/j.jvolgeores.2004.05.019.

Hildreth, W., 2017. Fluid-driven uplift at Long Valley Caldera, California: geologic perspectives. J. Volcanol. Geotherm. Res. 341, 269–286. https://doi.org/10.1016/j.jvolgeores.2017.06.010.

Hildreth, W., Fierstein, J., Calvert, A., 2017. Early postcaldera rhyolite and structural resurgence at Long Valley Caldera, California. J. Volcanol. Geotherm. Res. 335, 1–34. https://doi.org/10.1016/j.jvolgeores.2017.01.005.

Hildreth, W., Wilson, C.J.N., 2007. Compositional zoning of the bishop tuff. J. Petrol. 48, 951–999. https://doi.org/10.1093/petrology/egm007.

Hill, D.P., 2006. Unrest in long valley Caldera, California, 1978–2004. Geol. Soc. Spec. Publ. 269, 1–24. https://doi.org/10.1144/GSL.SP.2006.269.01.02.

Houghton, B.F., Wilson, C.J.N., McWilliams, M.O., Lanphere, M.A., Weaver, S.D., Briggs, R.M., Pringle, M.S., 1995. Chronology and dynamics of a large silicic magmatic system: central Taupo Volcanic Zone, New Zealand. Geology 23, 13–16.

Huber, C., Bachmann, O., Manga, M., 2009. Homogenization processes in silicic magma chambers by stirring and mushification (latent heat buffering). Earth Planet. Sci. Lett. 283, 38–47. https://doi.org/10.1016/j.epsl.2009.03.029.

Huber, C., Bachmann, O., Dufek, J., 2010. The limitations of melting on the reactivation of silicic mushes. J. Volcanol. Geotherm. Res. 195, 97–105. https://doi.org/10.1016/j.jvolgeores.2010.06.006.

Huber, C., Bachmann, O., Dufek, J., 2011. Thermo-mechanical reactivation of locked crystal mushes: melting-induced internal fracturing and assimilation processes in magmas. Earth Planet. Sci. Lett. 304, 443–454. https://doi.org/10.1016/j.epsl.2011.02.022.

Huber, C., Bachmann, O., Dufek, J., 2012. Crystal-poor versus crystal-rich ignimbrites: a competition between stirring and reactivation. Geology 40, 115–118. https://doi.org/10.1130/G32425.1.

Hughes, G.R., Mahood, G.A., 2008. Tectonic controls on the nature of large silicic calderas in volcanic arcs. Geology 36, 627–630. https://doi.org/10.1130/G24796A.1.

Jellinek, A.M., DePaolo, D.J., 2003. A model for the origin of large silicic magma chambers: precursors of caldera-forming eruptions. Bull. Volcanol. 65, 363–381. https://doi.org/10.1007/s00445-003-0277-y.

Jones, R.H., Stewart, R.C., 1997. A method for determining significant structures in a cloud of earthquakes. J. Geophys. Res. B Solid Earth 102, 8245–8254. https://doi.org/10.1029/96jb03739.

Jurado-Chichay, Z., Walker, G.P.L., 2000. Stratigraphy and dispersal of the Mangaone Subgroup pyroclastic deposits, Okataina volcanic centre, New Zealand. J. Volcanol. Geotherm. Res. 104, 319–380.

Justet, L., Spell, T.L., 2001. Effusive eruptions from a large silicic magma chamber: the Bearhead Rhyolite, Jemez volcanic field, NM. J. Volcanol. Geotherm. Res. 107, 241–264.

Kaneko, K., Kamata, H., Koyaguchi, T., Yoshikawa, M., Furukawa, K., 2007. Repeated large-scale eruptions from a single compositionally stratified magma chamber: an example from Aso volcano, Southwest Japan. J. Volcanol. Geotherm. Res. 167, 160–180.

Karakas, O., Degruyter, W., Bachmann, O., Dufek, J., 2017. Lifetime and size of shallow magma bodies controlled by crustal-scale magmatism. Nat. Geosci. 10, 446–450. https://doi.org/10.1038/ngeo2959.

Karlstrom, L., Dufek, J., Manga, M., 2009. Organization of volcanic plumbing through magmatic lensing by magma chambers and volcanic loads. J. Geophys. Res. Solid Earth 114, 1–16. https://doi.org/10.1029/2009JB006339.

Karlstrom, L., Dufek, J., Manga, M., 2010. Magma chamber stability in arc and continental crust. J. Volcanol. Geotherm. Res. 190, 249–270. https://doi.org/10.1016/j.jvolgeores.2009.10.003.

Karlstrom, L., Rudolph, M.L., Manga, M., 2012. Caldera size modulated by the yield stress within a crystal-rich magma reservoir. Nat. Geosci. 5, 402–405. https://doi.org/10.1038/ngeo1453.

Kay, S.M., Coira, B.L., Caffe, P.J., Chen, C.H., 2010. Regional chemical diversity, crustal and mantle sources and evolution of central Andean Puna plateau ignimbrites. J. Volcanol. Geotherm. Res. 198, 81–111. https://doi.org/10.1016/j.jvolgeores.2010.08.013.

Kelleher, P.C., Cameron, K.L., 1990. The geochemistry of the Mono Craters-Mono Lake Islands Volcanic Complex, Eastern California. J. Geophys. Res. 95 (B11), 17,643–17,659. https://doi.org/10.1029/JB095iB11p17643.

Kennedy, B., Wilcock, J., Stix, J., 2012. Caldera resurgence during magma replenishment and rejuvenation at Valles and Lake City calderas. Bull. Volcanol. 74, 1833–1847. https://doi.org/10.1007/s00445-012-0641-x.

Kilburn, C.R.J., De Natale, G., Carlino, S., 2017. Progressive approach to eruption at Campi Flegrei caldera in southern Italy. Nat. Commun. 8, 1–8.

Kiss, B., Harangi, S., Ntaflos, T., Mason, P.R.D., Pál-Molnár, E., 2014. Amphibole perspective to unravel pre-eruptive processes and conditions in volcanic plumbing systems beneath intermediate arc volcanoes: a case study from Ciomadul volcano (SE Carpathians). Contrib. Mineral. Petrol. 167, 1–27. https://doi.org/10.1007/s00410-014-0986-6.

Klemetti, E.W., Deering, C.D., Cooper, K.M., Roeske, S.M., 2011. Magmatic perturbations in the Okataina Volcanic Complex, New Zealand at thousand-year timescales recorded in single zircon crystals. Earth Planet. Sci. Lett. 305, 185–194. https://doi.org/10.1016/j.epsl.2011.02.054.

Knight, M.D., Walker, G.P.L., Ellwood, B.B., Diehl, J.F., 1986. Stratigraphy, paleomagnetism, and magnetic fabric of the Toba Tuffs: constraints on the sources and eruptive styles. J. Geophys. Res. 91, 10355. https://doi.org/10.1029/jb091ib10p10355.

Koyaguchi, T., Kaneko, K., 1999. A two-stage thermal evolution model of magmas in continental crust. J. Petrol. 40, 241–254. https://doi.org/10.1093/petroj/40.2.241.

Larson, R.L., Menard, H.W., Smith, S.M., 1968. Gulf of California: a result of ocean-floor spreading and transform faulting. Science 161 (80), 781–784.

Leonard, G.S., Begg, J.G., Wilson, C.J.N., 2010. Geology of the Rotorua area. Institute of Geological and Nuclear Sciences 1:250,000 Geological Map 5, Lower Hutt, New Zealand.

Lindsay, J.M., Schmitt, A.K., Trumbull, R.B., De Silva, S.L., Siebel, W., Emmermann, R., 2001. Magmatic evolution of the La Pacana Caldera system, Central Andes, Chile: compositional variation of two cogenetic, large-volume felsic ignimbrites. J. Petrol. 42, 459–486. https://doi.org/10.1093/petrology/42.3.459.

Lipman, P.W., 1984. The roots of ash flow calderas in western North America: windows into the tops of granitic batholiths. J. Geophys. Res. 89, 8801–8841. https://doi.org/10.1029/JB089iB10p08801.

Lipman, P.W., 2000. Calderas. In: Encyclopedia of Volcanoes, pp. 643–662.

Lipman, P.W., Zimmerer, M.J., mcintosh, W.C., 2015. An ignimbrite caldera from the bottom up: exhumed floor and fill of the resurgent Bonanza caldera, Southern Rocky Mountain volcanic field, Colorado. Geosphere 11, 1902–1947. https://doi.org/10.1130/GES01184.1.

Lowenstern, J.B., 2000. A review of the contrasting behavior of two magmatic volatiles: chlorine and carbon dioxide. J. Geochem. Explor. 69, 287–290.

Lowenstern, J.B., Smith, R.B., Hill, D.P., 2006. Monitoring super-volcanoes: geophysical and geochemical signals at Yellowstone and other large caldera systems. Philos. Trans. R. Soc. A Math. Phys. Eng. Sci. 364, 2055–2072.

Malfait, W.J., Seifert, R., Petitgirard, S., Perrillat, J.P., Mezouar, M., Ota, T., Nakamura, E., Lerch, P., Sanchez-Valle, C., 2014. Supervolcano eruptions driven by melt buoyancy in large silicic magma chambers. Nat. Geosci. 7, 122–125. https://doi.org/10.1038/ngeo2042.

Manning, D.A., 1996. Middle-Late Pleistocene Tephrostratigraphy of the Eastern Bay of Plenty, New Zealand. Quat. Int. 34–36, 3–12.

Marsh, B.D., 1981. On the crystallinity, probability of occurrence, and rheology of lava and magma. Contrib. Mineral. Petrol. 78, 85–98.

Marsh, B.D., 1984. On the mechanics of Caldera resurgence. J. Geophys. Res. 89, 8245–8251.

Matthews, N.E., Huber, C., Pyle, D.M., Smith, V.C., 2012. Timescales of magma recharge and reactivation of large silicic systems from ti diffusion in quartz. J. Petrol. 53, 1385–1416. https://doi.org/10.1093/petrology/egs020.

McKee, C.O., Duncan, R.A., 2016. Early volcanic history of the Rabaul area. Bull. Volcanol. 78 https://doi.org/10.1007/s00445-016-1018-3.

McKee, C.O., Fabbro, G.N., 2018. The Talili Pyroclastics eruption sequence: VEI 5 precursor to the seventh century CE caldera-forming event at Rabaul, Papua New Guinea. Bull. Volcanol. 80, 1–28. https://doi.org/10.1007/s00445-018-1255-8.
McKee, C.O., Baillie, M.G., Reimer, P.J., 2015. A revised age of ad 667–699 for the latest major eruption at Rabaul. Bull. Volcanol. 77, 1–7. https://doi.org/10.1007/s00445-015-0954-7.
Mckee, C., Itikarai, I., Kuduon, J., Lauer, N., Lolok, D., Patia, H., Ours, P.D. Saint, 2018. Independent State of Papua New Guinea Geohazards Management. The 1994–1998 Eruptions at Rabaul: Main Features and Analysis.
Metz, J.M., Mahood, G.A., 1985. Precursors to the Bishop Tuff eruption: Glass Mountain, Long Valley, California (USA). J. Geophys. Res. 90 https://doi.org/10.1029/jb090ib13p11121.
Metz, J.M., Mahood, G.A., 1991. Development of the Long Valley, California, magma chamber recorded in precaldera rhyolite lavas of Glass Mountain. Contrib. Mineral. Petrol. 106, 379–397. https://doi.org/10.1007/BF00324565.
Michaut, C., Jaupart, C., 2006. Ultra-rapid formation of large volumes of evolved magma. Earth Planet. Sci. Lett. 250, 38–52. https://doi.org/10.1016/j.epsl.2006.07.019.
Moore, J.G., Dodge, F.C.W., 1980. Late Cenozoic volcanic rocks of the southern Sierra Nevada, California: I. Geology and petrology. Geol. Soc. Am. Bull. 91, 1995–2038. https://doi.org/10.1017/CBO9781107415324.004.
Mucek, A.E., Danišík, M., De Silva, S.L., Schmitt, A.K., Pratomo, I., Coble, M.A., 2017. Post-supereruption recovery at Toba Caldera. Nat. Commun. 8 https://doi.org/10.1038/ncomms15248.
Muller, J.R., Ito, G., Martel, S.J., 2001. Effects of volcano loading on dike propagation in an elastic half-space. J. Geophys. Res. Solid Earth 106, 11101–11113. https://doi.org/10.1029/2000jb900461.
Nairn, I.A., 2002. Geology of the Okataina Volcanic Centre.
Nairn, I.A., Talai, B., Wood, C.P., McKee, C.O., 1989. Rabaul Caldera, Papua New Guinea—1: 25,000 reconnaissance geological map and eruption history. In: Rep. Prep. Minist. Extern. Relations Trade, New Zeal, pp. 1–75.
Nairn, I.A., Mckee, C.O., Talai, B., Wood, C.P., 1995. Geology and eruptive history of the Rabaul Caldera area, Papua New Guinea. J. Volcanol. Geotherm. Res. 69, 255–284. https://doi.org/10.1016/0377-0273(95)00035-6.
Nairn, I.A., Shane, P.R., Cole, J.W., Leonard, G.J., Self, S., Pearson, N., 2004. Rhyolite magma processes of the ~AD 1315 Kaharoa eruption episode, Tarawera volcano, New Zealand. J. Volcanol. Geotherm. Res. 131, 265–294. https://doi.org/10.1016/S0377-0273(03)00381-0.
Newhall, C.G., Dzurisin, D., 1988. Historical Unrest at the Large Calderas of the World, US Geological Survey Bulletin. Department of the Interior, US Geological Survey.
Orsi, G., Civetta, L., D'Antonio, M., Di Girolamo, P., Piochi, M., 1995. Step-filling and development of a three-layer magma chamber: the Neapolitan Yellow Tuff case history. J. Volcanol. Geotherm. Res. 67, 291–312. https://doi.org/10.1016/0377-0273(94)00119-2.
Pansino, S., Taisne, B., 2019. How magmatic storage regions attract and repel propagating dikes. J. Geophys. Res. Solid Earth 124, 274–290. https://doi.org/10.1029/2018JB016311.
Pappalardo, L., Civetta, L., D'Antonio, M., Deino, A., Di Vito, M., Orsi, G., Carandente, A., De Vita, S., Isaia, R., Piochi, M., 1999. Chemical and Sr-isotopical evolution of the Phlegraean magmatic system before the Campanian Ignimbrite and the Neapolitan Yellow Tuff eruptions. J. Volcanol. Geotherm. Res. 91, 141–166. https://doi.org/10.1016/S0377-0273(99)00033-5.
Parmigiani, A., Faroughi, S., Huber, C., Bachmann, O., Su, Y., 2016. Bubble accumulation and its role in the evolution of magma reservoirs in the upper crust. Nature 532, 492–495. https://doi.org/10.1038/nature17401.
Parmigiani, A., Degruyter, W., Leclaire, S., Huber, C., Bachmann, O., 2017. The mechanics of shallow magma reservoir outgassing. Geochem. Geophys. Geosyst. 18, 2887–2905. https://doi.org/10.1002/2017GC006912.
Patia, H., Eggins, S.M., Arculus, R.J., McKee, C.O., Johnson, R.W., Bradney, A., 2017. The 1994–2001 eruptive period at Rabaul, Papua New Guinea: petrological and geochemical evidence for basalt injections into a shallow dacite magma reservoir, and significant SO2 flux. J. Volcanol. Geotherm. Res. 345, 200–217. https://doi.org/10.1016/j.jvolgeores.2017.08.011.
Pearce, N.J.G., Westgate, J.A., Gualda, G.A.R., Gatti, E., Muhammad, R.F., 2020. Tephra glass chemistry provides storage and discharge details of five magma reservoirs which fed the 75 ka Youngest Toba Tuff eruption, northern Sumatra. J. Quat. Sci. 35, 256–271. https://doi.org/10.1002/jqs.3149.
Pe-Piper, G., Moulton, B., 2008. Magma evolution in the Pliocene-Pleistocene succession of Kos, South Aegean arc (Greece). Lithos 106, 110–124. https://doi.org/10.1016/j.lithos.2008.07.002.
Pe-Piper, G., Piper, D.J.W., Perissoratis, C., 2005. Neotectonics and the Kos Plateau Tuff eruption of 161 ka, South Aegean arc. J. Volcanol. Geotherm. Res. 139, 315–338. https://doi.org/10.1016/j.jvolgeores.2004.08.014.
Piper, D.J.W., Pe-Piper, G., Lefort, D., 2010. Precursory activity of the 161 ka Kos Plateau Tuff eruption, Aegean Sea (Greece). Bull. Volcanol. 72, 657–669. https://doi.org/10.1007/s00445-010-0349-8.
Popa, R.G., Bachmann, O., Ellis, B.S., Degruyter, W., Tollan, P., Kyriakopoulos, K., 2019. A connection between magma chamber processes and eruptive styles revealed at Nisyros-Yali volcano (Greece). J. Volcanol. Geotherm. Res. 387 https://doi.org/10.1016/j.jvolgeores.2019.106666.
Popa, R.G., Guillong, M., Bachmann, O., Szymanowski, D., Ellis, B., 2020. U-Th zircon dating reveals a correlation between eruptive styles and repose periods at the Nisyros-Yali volcanic area, Greece. Chem. Geol. 555, 119830. https://doi.org/10.1016/j.chemgeo.2020.119830.
Putirka, K.D., 2008. Thermometers and barometers for volcanic systems. Rev. Mineral. Geochem. 69 (1), 61–120. https://doi.org/10.2138/rmg.2008.69.3.
Rivalta, E., Corbi, F., Passarelli, L., Acocella, V., Davis, T., Di Vito, M.A., 2019. Stress inversions to forecast magma pathways and eruptive vent location. Sci. Adv. 5, 1–12. https://doi.org/10.1126/sciadv.aau9784.
Roggensack, K., Williams, S.N., Schaefer, S.J., Parnell, R.A., 1996. Volatiles from the 1994 eruptions of Rabaul: understanding large caldera systems. Science 273 (80), 490–493. https://doi.org/10.1126/science.273.5274.490.
Rubin, A., Cooper, K.M., Leever, M., Wimpenny, J., Deering, C., Rooney, T., Gravley, D., Yin, Q. Zhu, 2016. Changes in magma storage conditions following caldera collapse at Okataina Volcanic Center, New Zealand. Contrib. Mineral. Petrol. 171, 1–18. https://doi.org/10.1007/s00410-015-1216-6.
Sable, J.E., Houghton, B.F., Wilson, C.J.N., Carey, R.J., 2006. Complex proximal sedimentation from Plinian plumes: the example of Tarawera 1886. Bull. Volcanol. 69, 89.
Sampson, D.E., Cameron, K.L., 1987. The geochemistry of the Inyo Volcanic Chain: Multiple magma systems in the Long Valley Region, eastern California. J. Geophys. Res. 92 (B10), 10403–10421. https://doi.org/10.1029/JB092iB10p10403.
Scandone, P., Patacca, E., 1984. Tectonic evolution of the Central Mediterranean area. Ann. Geophys. 2, 139–142.
Self, S., Rampino, M.R., 1981. The 1883 eruption of Krakatau. Nature 294, 699–704. https://doi.org/10.1038/294699a0.
Self, S., Rampino, M.R., Newton, M.S., Wolff, J.A., 1984. Volcanological study of the great Tambora eruption of 1815. Geology 12, 659–663.
Shane, P., Smith, V.C., 2013. Using amphibole crystals to reconstruct magma storage temperatures and pressures for the post-caldera collapse volcanism at Okataina volcano. Lithos 156–159, 159–170. https://doi.org/10.1016/j.lithos.2012.11.008.
Shane, P., Nairn, I.A., Smith, V.C., 2005. Magma mingling in the ~50 ka Rotoiti eruption from Okataina Volcanic Centre: implications for geochemical diversity and chronology of large volume rhyolites. J. Volcanol. Geotherm. Res. 139, 295–313. https://doi.org/10.1016/j.jvolgeores.2004.08.012.
Sheldrake, T., Caricchi, L., Scutari, M., 2020. Tectonic controls on global variations of large-magnitude explosive eruptions in volcanic arcs. Front. Earth Sci. 8, 1–14. https://doi.org/10.3389/feart.2020.00127.
Shinohara, H., 1994. Exsolution of immiscible vapor and liquid phases from a crystallizing silicate melt: implications for chlorine and metal transport. Geochim. Cosmochim. Acta 58, 5215–5221. https://doi.org/10.1016/0016-7037(94)90306-9.
Sieh, K., Bursik, M., 1986. These Rhyolitic Sieh and Bursik: Eruption of Mono, p. 91.
Sliwinski, J.T., Bachmann, O., Dungan, M.A., Huber, C., Deering, C.D., Lipman, P.W., Martin, L.H.J., Liebske, C., 2017. Rapid pre-eruptive thermal rejuvenation in a large silicic magma body: the case of the Masonic Park Tuff, Southern Rocky Mountain volcanic field, CO, USA. Contrib. Mineral. Petrol. 172, 30.
Smith, R.L., Bailey, R.A., 1968. Resurgent cauldrons. Mem. Geol. Soc. Am. 116, 613–662. https://doi.org/10.1130/MEM116-p613.
Smith, V.C., Isaia, R., Pearce, N.J.G., 2011. Tephrostratigraphy and glass compositions of post-15 kyr Campi Flegrei eruptions: implications for eruption history and chronostratigraphic markers. Quat. Sci. Rev. 30 (25–26), 3638–3660. https://doi.org/10.1016/j.quascirev.2011.07.012.
Smith, P.E., York, D., Chen, Y., Evensen, N.M., 1996. Single crystal 40Ar-39Ar dating of a Late Quaternary paroxysm on Kos, Greece: concordance of terrestrial and marine ages. Geophys. Res. Lett. 23, 3047–3050.
St Seymour, K.S., Vlassopoulos, D., 1992. Journal of Volcanology and Geothermal Research Volume 50 issue 3 1992 [doi 10.1016%2F0377-0273%2892%2990097-w] Karen St. Seymour; Dimitri Vlassopoulos – Magma mixing at Nisyros volcano, as inferred from incompatible.pdf 50, 273–299.
Spandler, C., Martin, L.H.J., Pettke, T., 2012. Carbonate assimilation during magma evolution at Nisyros (Greece), South Aegean Arc: evidence from clinopyroxenite xenoliths. Lithos 146, 18–33. https://doi.org/10.1016/j.lithos.2012.04.029.
Stix, J., Layne, G.D., 1996. Gas saturation and evolution of volatile and light lithophile elements in the Bandelier magma chamber between two caldera-forming eruptions. J. Geophys. Res. Solid Earth 101, 25181–25196. https://doi.org/10.1029/96jb00815.
Stock, M.J., Humphreys, M.C.S., Smith, V.C., Isaia, R., Pyle, D.M., 2016. Late-stage volatile saturation as a potential trigger for explosive volcanic eruptions. Nat. Geosci. 9, 249–254.
Storm, S., Shane, P., Schmitt, A.K., Lindsay, J.M., 2011. Contrasting punctuated zircon growth in two syn-erupted rhyolite magmas from Tarawera volcano: insights to crystal diversity in magmatic systems. Earth Planet. Sci. Lett. 301, 511–520. https://doi.org/10.1016/j.epsl.2010.11.034.
Suzuki-Kamata, K., Kamata, H., Bacon, C.R., 1993. Evolution of the caldera-forming eruption at Crater Lake, Oregon, indicated by component analysis of lithic fragments. J. Geophys. Res. Solid Earth 98, 14059–14074.
Thompson, A.B., Matile, L., Ulmer, P., 2002. Some thermal constraints on crustal assimilation during fractionation of hydrous, mantle-derived magmas with examples from Central Alpine Batholiths. J. Petrol. 43, 403–422. https://doi.org/10.1093/petrology/43.3.403.
Townsend, M., Huber, C., 2020. A critical magma chamber size for volcanic eruptions. Geology 48, 431–435. https://doi.org/10.1130/G47045.1.
Townsend, M., Huber, C., Degruyter, W., Bachmann, O., 2019. Magma chamber growth during Intercaldera periods: insights from thermo-mechanical modeling with applications to Laguna del Maule, Campi Flegrei, Santorini, and Aso. Geochem. Geophys. Geosyst. 20, 1574–1591. https://doi.org/10.1029/2018GC008103.
Tregoning, P., Jackson, R.J., McQueen, H., Lambeck, K., Stevens, C., Little, R.P., Curley, R., Rosa, R., 1999. Motion of the South Bismarck Plate, Papua New Guinea. Geophys. Res. Lett. 26, 3517–3520.
Troch, J., Ellis, B.S., Mark, D.F., Bindeman, I.N., Kent, A.J.R., Guillong, M., Bachmann, O., 2017. Rhyolite generation prior to a yellowstone supereruption:

insights from the Island Park-Mount Jackson rhyolite series. J. Petrol. 58, 29–52. https://doi.org/10.1093/petrology/egw071.
Van Kooten, G.K., 1980. Mineralogy, petrology, and geochemistry of an ultrapotassic basaltic suite, central Sierra Nevada, California, USA. J. Petrol. 21 (4), 651–684. https://doi.org/10.1093/petrology/21.4.651.
Volentik, A., Vanderkluysen, L., Principe, C., Hunziker, J.C., 2005. Stratigraphy of Nisyros Volcano (Greece). In: Hunziker, J.C., Marini, L. (Eds.), The Geology, Geochemistry and Evolution of Nisyros Volcano (Greece): Implications for the Volcanic Hazards. Université de Lausanne, Lausanne, p. 192.
Vougioukalakis, G.E., 1993. Volcanic stratigraphy and evolution of Nisyros Island. Bull. Geol. Soc. Greece 28, 239–258.
Wallace, P.J., Anderson, A.T., Davis, A.M., 1999. Gradients in H2O, CO2, and exsolved gas in a large-volume silicic magma system: interpreting the record preserved in melt inclusions from the Bishop Tuff. J. Geophys. Res. Solid Earth 104, 20097–20122. https://doi.org/10.1029/1999jb900207.
Ward, P.L., 1991. On plate tectonics and the geologic evolution of southwestern North America. J. Geophys. Res. Solid Earth 96, 12479–12496.
Wark, D.A., Hildreth, W., Spear, F.S., Cherniak, D.J., Watson, E.B., 2007. Pre-eruption recharge of the Bishop magma system. Geology 35, 235–238. https://doi.org/10.1130/G23316A.1.
Waters, L.E., Lange, R.A., 2015. An updated calibration of the plagioclase-liquid hygrometer-thermometer applicable to basalts through rhyolites. Am. Mineral. 100 (10), 2172–2184. https://doi.org/10.2138/am-2015-5232.
Watts, K.E., John, D.A., Colgan, J.P., Henry, C.D., Bindeman, I.N., Schmitt, A.K., 2016. Probing the volcanic-plutonic connection and the genesis of crystal-rich rhyolite in a deeply dissected supervolcano in the Nevada Great Basin: source of the late Eocene Caetano Tuff. J. Petrol. 57, 1599–1644. https://doi.org/10.1093/petrology/egw051.
Webster, J.D., 1997. Chloride solubility in felsic melts and the role of chloride in magmatic degassing. J. Petrol. 38, 1793–1807. https://doi.org/10.1093/petroj/38.12.1793.
Webster, J.D., 2004. The exsolution of magmatic hydrosaline chloride liquids. Chem. Geol. 210, 33–48. https://doi.org/10.1016/j.chemgeo.2004.06.003.
Williams, S.N., 1995. Stanley N. Williams, 267, pp. 340–341.
Wilson, C.J.N., Houghton, B.F., McWilliams, M.O., Lanphere, M.A., Weaver, S.D., Briggs, R.M., 1995. Volcanic and structural evolution of Taupo Volcanic Zone, New Zealand: a review. J. Volcanol. Geotherm. Res. 68, 1–28. https://doi.org/10.1016/0377-0273(95)00006-G.
Wolff, J.A., Ellis, B.S., Ramos, F.C., Starkel, W.A., Boroughs, S., Olin, P.H., Bachmann, O., 2015. Remelting of cumulates as a process for producing chemical zoning in silicic tuffs: a comparison of cool, wet and hot, dry rhyolitic magma systems. Lithos 236–237, 275–286. https://doi.org/10.1016/j.lithos.2015.09.002.
Wolff, J.A., Forni, F., Ellis, B.S., Szymanowski, D., 2020. Europium and barium enrichments in compositionally zoned felsic tuffs: a smoking gun for the origin of chemical and physical gradients by cumulate melting. Earth Planet. Sci. Lett. 540, 116251. https://doi.org/10.1016/j.epsl.2020.116251.
Wood, C.P., Nairn, I.A., Mckee, C.O., Talai, B., 1995. Petrology of the Rabaul Caldera area, Papua New Guinea. J. Volcanol. Geotherm. Res. 69, 285–302. https://doi.org/10.1016/0377-0273(95)00034-8.
Wyers, G.P., Barton, M., 1989. Polybaric evolution of calc-alkaline magmas from nisyros, southeastern hellenic arc, Greece. J. Petrol. 30, 1–37. https://doi.org/10.1093/petrology/30.1.1.
Zellmer, G.F., Turner, S.P., 2007. Arc dacite genesis pathways: evidence from mafic enclaves and their hosts in Aegean lavas. Lithos 95, 346–362. https://doi.org/10.1016/j.lithos.2006.08.002.